DIRECT DISPLACEMENT BASED DESIGN OF R/C STRUCTURAL WALLS

by

Ali Bozer

B.S. in C.E., Yıldız Technical University, 1999

Submitted to the Institute for Graduate Studies in
Science and Engineering in partial fulfillment of
the requirements for the degree of
Master of Science
in
Civil Engineering

Boğaziçi University

2003

ACKNOWLEDGEMENTS

Life is made up of choices, paths of variety and I owe a lot to Prof. Gülay ALTAY for she directs me to trail the right. Thus I would like to express my greatest thanks to her for not only being a supervisor but also a mentor to me.

I would also like to thank to my friends and colleagues whom I walk with. I always felt their shield of support and encouragement against the blows of life.

Lastly, I feel grateful and lucky to have such a family. Their help and support is beyond the power of words. This thesis is dedicated to them.

ABSTRACT

DIRECT DISPLACEMENT BASED DESIGN OF R/C STRUCTURAL WALLS

It is known that the conventional code based design has some drawbacks in estimating actual structure performance which stems from inconsistency between assumed force reduction factors and actual ductility demand as well as the utilization of gross section stiffness which ends up with significant errors in estimation of yield displacement. As a consequence, conventional code based designs are generally very conservative and actual structure performance is left unknown unless a more detailed analysis is performed.

The object of this study is to review direct displacement based design methodology and to introduce an alternative approach for assessment of target displacement profile and effective damping ratio. This modified direct displacement based design enables one to design a structure for the selected performance level since the controlling design input is plastic hinge rotations which can be taken from ATC 40 for various performance levels. In this design methodology seismic design is performed by identifying a target displacement profile which is a function of plastic hinge rotation, section dimensions and reinforcement details used. Strength and stiffness are not the variables in the procedure but they are the end results.

A series of moment-curvature and push over analyses were performed to verify design outputs for various structural wall sections. It is seen that the design plastic rotations as well as the target displacements are in conformity with the ones obtained from the analyses.

ÖZET

BETONARME PERDE DUVARLARIN DİREKT DEPLASMAN BAZLI TASARIMI

Mevcut yönetmelikte kullanılan tasarım yönteminin önerdiği deprem azaltma katsayıları ve gerçek düktilite talebi arasındaki tutarsızlıktan, bunun yanında elastik deplasmanının seçiminde önemli hatalara sebebiyet verebilen rijitlik hesaplarında bürüt alan kullanılmasından doğan bir takım dezavantajlarının olduğu bilinmektedir. Sonuç olarak, yönetmeliğin önerdiği klasik tasarımlar genellikle çok konservatif olmakta ve daha detaylı bir analiz yapılmadıkça gerçek yapı performansı bilinememektedir.

Bu çalışmanın amacı, direkt deplasman bazlı tasarım metodunu incelemek aynı zamanda hedef deplasman profili ve etkin sönüm oranının hesabı için alternatif bir yaklaşım sunmaktır. Bu modifiye edilmiş direkt deplasman bazlı tasarım yönteminde limit dizayn girdisi değişik performans seviyeleri için ATC40'den alınabilecek plastik mafsal dönmeleri olduğu için istenilen performans seviyesinde dizaynı mümkün kılmaktadır. Bu dizayn metodunda deprem hesabı plastik mafsal dönmeleri, kesit boyutları ve kullanılan donatı detayının bir fonksiyonu olan hedef deplasman profilinin tanımlanmasıyla gerçekleştirilir. Dayanım ve rijitlik dizayn değişkenleri değil fakat sonuçlarıdır.

Değişik kesitlerdeki perde duvarların dizayn sonuçlarının değerlendirilebilmesi için moment-eğrilik ve yanal itme analizleri uygulanmıştır. Bu analizlerin sonucunda dizayn plastik dönmelerinin ve hedef deplasmanların analizlerle uygunluk içinde olduğu görülmüştür.

TABLE OF CONTENTS

LIST OF FIGURES

LIST OF TABLES

LIST OF SYMBOLS / ABBREVIATIONS

A_o	Effective ground acceleration coefficient
B_L	Damping coefficient for long period
B_S	Damping coefficient for short period
d_{bl}	Longitudinal bar diameter
E	Modulus of elasticity for reinforced concrete
E_D	Energy dissipated by damping
E_{So}	Maximum strain energy
f_y	Longitudinal bar yield stress
h_i	Structural wall height at i^{th} storey
h_w	Structural wall height
I	Moment of inertia for reinforced concrete
I_{eff}	Effective moment of inertia for reinforced concrete
I_g	Gross section moment of inertia for reinforced concrete
K_{eff}	Effective stiffness
L_p	Plastic hinge length
l_w	Structural wall length
M_{eff}	Effective participating mass
MF	Modification factor
M_p	Total moment of structural wall when the system is displaced to performance point
M_y	Yield moment of structural wall
R_{3py}	Post-yield rotational stiffness for NLLink element
R_{3y}	Pre-yield rotational stiffness for NLLink element
r	Slope ratio
S_a	Spectral acceleration
S_d	Spectral displacement
T_A, T_B	Spectrum characteristic periods
T_{eff}	Effective period
$T_{5\%}$	Period at 5 per cent damping
T_ζ	Period at damping value ζ

V_d	Design base shear
V_u	Ultimate base shear
α	Amplification factor for push-over steps
β_{eff}	Effective viscous damping
β_{eq}	Equivalent viscous damping
β_o	Hysteretic damping
Δ_{ei}	Elastic displacement profile
Δ_i	Total displacement profile
Δ_{pi}	Plastic displacement profile
Δ_{sys}	Target spectral displacement
Δ_t	Target displacement
Δ_u	Ultimate displacement
Δ_y	Yield displacement
γ_n	First mode participation factor for top displacement
κ	Damping modification factor
μ	Displacement ductility ratio
$\emptyset_y$	Structural wall yield curvature
Ψ_1	First mode shape for the building
θ_e	Elastic rotation at plastic zone
θ_{et}	Top storey elastic rotation
θ_{lim}	UBC drift ratio / Rotational limit
θ_p	Plastic rotation at plastic zone
θ_T	Total rotation at plastic zone
ζ	Effective damping
ADRS	Acceleration-Displacement Response Spectra
ATC	Applied Technology Council
DDBD	Direct displacement based design
NLLink	Nonlinear link
UBC	Uniform Building Code

1. INTRODUCTION

1.1. General

For the last several decades, force based design is utilized to perform seismic design in which a pseudo lateral force is applied to the linearly elastic model of the building, resulting in design displacement amplitudes approximating maximum displacements expected during design earthquake. In the codified design approach the elastic stiffness of reinforced concrete members is established from first principles of structural mechanics, using geometric properties of members and the modulus of elasticity for the material. However, if the building responds inelastically to the design earthquake, as it is the majority of the cases, stiffness is reduced due to the extent and influence of cracking in the members as well as reduction in effective modulus of steel. This conflict leads to gross errors in deformation assessment and makes control of performance impossible unless a more detailed analysis is performed. Also response is taken at the instance of peak base shear for an equivalent elastically responding structure. The effect of pinched hysteretic shape, stiffness degradation and strength deterioration on maximum displacement response is not considered especially when the structure undergoes to high number of response cycles.

Results of dynamic tests of reinforced concrete frames show that when a structure undergoes a seismic attack, together with the reduced stiffness its energy dissipation capacity increases. The area within a cycle of the force-displacement curve is a measure of energy dissipated by the vibrating system in that cycle and when earthquake excites structure into larger inelastic displacements, the area within the hysteresis loop increases. This energy dissipation mechanism is directly related to ductility attained by the structure, so it can be defined as hysteretic damping. Therefore, an effective damping as a combination of viscous damping that is inherent in the structure and hysteretic damping substituted viscous damping. By following this logic Gülkan and Sözen approximated single degree of freedom systems by linear response analysis using a reduced stiffness and a substitute damping related to hysteretic properties of reinforced concrete. By using the concept of reduced stiffness and substitute damping he utilized a procedure based on linear

response to estimate effects of inelastic response for single-degree-of-freedom reinforced concrete structures [1]. The procedure involves an assumption of ductility, and then substitute damping ratio is derived by using Takeda's hysteresis model [2]. Base shear and maximum displacement is obtained by entering increased natural period to spectral response diagram corresponding to substitute damping ratio calculated.

The substitute-structure method extended this procedure to multi degree of freedom systems [3]. The method enabled one to consider displacements in design process and allowed the use of linear-response models for nonlinear dynamic analysis but the true power of the method was the choice of various deformation levels to different elements of the structure. By doing so, a designer gains an extent control not only in global structure response as in conventional code design but also deformation pattern. For example strong column-weak beam criteria could be explicitly controlled by setting different deformation limits to columns and beams in substitute-structure method.

Reduction factors used in conventional code design are made up of two parameters: Over strength factor and ductility. If we assume that the over strength factor is constant then force reduction factors are related to ductility. However, generalized prediction of system ductility may not be consistent with one of an individual system since static system, stiffness and strength characteristics and redistribution of forces play important role in determining system ductility. Although setting ductility on element level is a progress, the same problem is also valid for substitute-structure method. Accurate selection of ductility depends on proper estimation of yield displacement profile together with target displacement profile however, for multi degree of freedom frame systems estimation of displacement profile is rather difficult for; prediction of possible plastic zones is complex due to force redistribution. So, for accurate design the methodology is bound to single degree of freedom systems or multi degree of freedom systems at which the location of plastic zones are strictly known as in the case of cantilever structural walls or cantilever bridge columns.

Kowalsky *et al.* utilized the substitute structure approach, and developed a displacement based design methodology for reinforced concrete bridge columns [4]. The procedure is based on an initial guess of ductility and verification of this ductility through

an iterative process. In 2001 Kowalsky proposed direct displacement based design methodology [5] in which the application area is cantilever structural walls, and ductility is directly found through a mathematical model enabling one to calculate yield and target displacement profiles of cantilever structural walls.

The objective of this thesis is to investigate and to suggest some modifications to the mathematical model proposed by Kowalsky for estimating the two key parameters in direct displacement based design, which are target displacement profile and effective damping.

1.2. Direct Displacement Based Design Procedure

Displacement-based design methodology enables engineer to select the design performance level for the building and provides reliable designs while retaining simplicity in the design process. The core of the design process is the selection of the target displacement which is intended to represent the maximum displacement likely to be experienced during the design earthquake. Because the mathematical model accounts for effects of material inelastic response, the calculated internal forces will be reasonable approximations of those expected during the design earthquake.

Two basic characteristics of reinforced concrete play an important role in determining response to strong ground motions. They are the change in stiffness and energy dissipation capacity. Both can be related to the maximum displacement. As earthquake motion influence larger displacements to the structure, its stiffness decreases and its capacity to dissipate energy increases due to the increase in area within the hysteresis loop.

The direct displacement-based design procedure acknowledges these two basic characteristics of reinforced concrete and utilizes an equivalent elastic system as a model for inelastic system. The equivalent elastic system is known as the substitute structure and has properties:

i. Effective Stiffness, K_{eff}

ii. Effective Damping, ζ

iii. Effective Period, T_{eff}

In direct displacement-based design procedure, a target displacement is specified and yield displacement is estimated. As being a function of displacement ductility, the effective damping is calculated. By entering the target displacement to the displacement spectra which is reduced in proportion to effective damping, the effective period is read. The effective period is then expressed as an effective stiffness from consideration of SDOF oscillator. The design base shear is obtained by the product of the effective stiffness and target displacement.

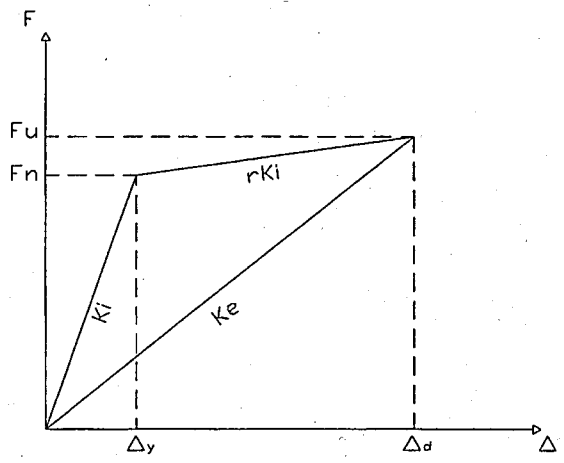

Figure 1.1. Substitute structure approach

1.2.1. Target Displacement Profile

The target displacement profile for the displacement-based design procedure is based on the UBC drift limit of $\theta_{lim} = 0.02$ or 0.025, depending on the fundamental period of vibration of the building. Plastic hinge length L_p is calculated by the greater of the values of (1.1) and (1.2) [6].

$$L_p = 0.2l_w + 0.044\left(\frac{2}{3}h_w\right) \qquad (1.1)$$

$$L_p = 0.08\left(\frac{2}{3}h_w\right) + 0.022 f_y d_{bl} \tag{1.2}$$

Where, h_w is wall height, l_w is wall length, f_y is longitudinal bar yield stress and d_{bl} is longitudinal bar diameter. The displacement profile, Δ_i, is obtained by (1.3) where the elastic profile, Δ_{ei}, is given by (1.4), and the plastic profile, Δ_{pi}, is given by (1.5)

$$\Delta_i = \Delta_{ei} + \Delta_{pi} \tag{1.3}$$

$$\Delta_{ei} = \frac{\phi_y h_i^2}{3}\left(1.5 - \frac{h_i}{h_w}\right) \tag{1.4}$$

$$\Delta_{pi} = \left(\theta_{\text{lim}} - \theta_{et}\right)\left(h_i - \frac{L_p}{2}\right) \tag{1.5}$$

In (1.4), ϕ_y is the wall yield curvature and is given by (1.5) assuming that the neutral axis depth is the half of the wall length.

$$\phi_y = 2\epsilon_y / l_w \tag{1.6}$$

In (1.5), θ_{et} is the top-story elastic rotation which is shown in (1.7)

$$\theta_{et} = \frac{\phi_y h_w}{2} \tag{1.7}$$

1.2.2. Effective Damping

The percentage of equivalent viscous damping is given by (1.8) [4] where μ_Δ is the displacement ductility demand. Equation (1.8) is based on the Takeda [2] degrading stiffness hysteretic response and includes 5 per cent viscous damping component and the effective damping component based on hysteretic energy dissipation.

For buildings with equal length walls, the effective damping of the building is the effective damping of any given wall. For buildings with unequal wall lengths, the ductility hence damping will vary for each wall. As a result, the effective damping for the building is obtained by combining the individual wall effective damping values in proportion to the work done by each wall.

$$\zeta = 100\left(0.05 + \frac{1 - \frac{0.95}{\sqrt{\mu_\Delta}} - 0.05\sqrt{\mu_\Delta}}{\pi}\right) \tag{1.8}$$

1.2.3. Design Base Shear

The seismic input for Direct Displacement-Based Design is expressed in the form of displacement response spectra (DRS). The spectral values for the DRS is obtained by multiplying acceleration response spectra (ARS) values by $T^2 / 4\pi^2$. For Direct Displacement-Based Design response spectra for damping values greater than 5 per cent are required. EuroCode 8 (CEC 1988) relation (1.9) relates the spectral displacement response, Δ_ζ ,at a damping value of ζ to the spectral displacement response at 5 per cent damping. In (1.9), ζ is expressed in per cent.

$$\Delta_\zeta = \Delta_{5\%}\left(\frac{7}{2+\zeta}\right)^{1/2} \tag{1.9}$$

As can be seen from the displacement response spectrum for 5 per cent damping in Figure 1.2 can be assumed as linear. So, by using a linear displacement response spectrum, period at damping values other than 5 per cent is calculated. The procedure is shown in the following pages.

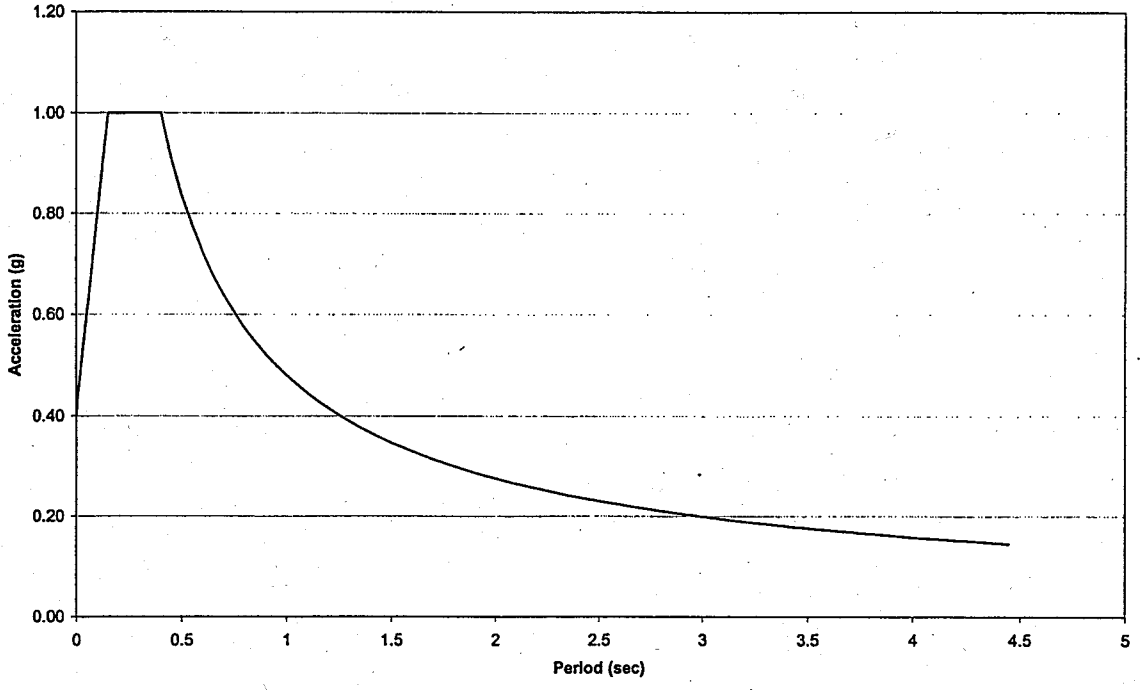

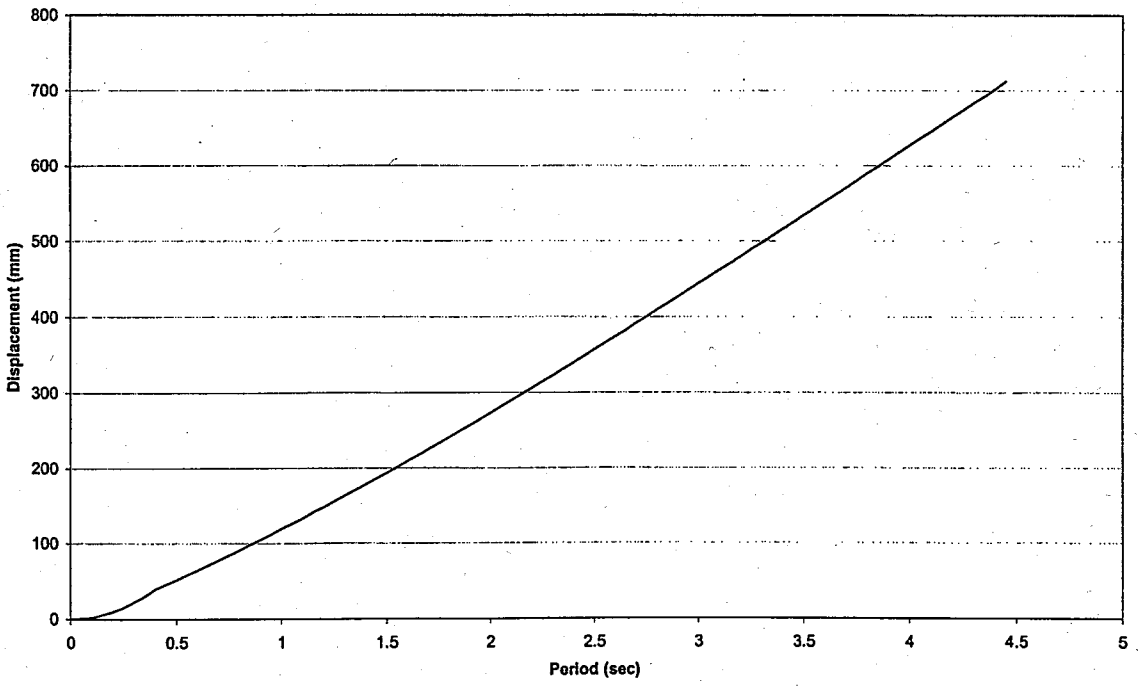

Figure 1.2. (a) Acceleration Response Spectrum for 5 per cent damping (b) Displacement Response Spectrum for 5 per cent damping

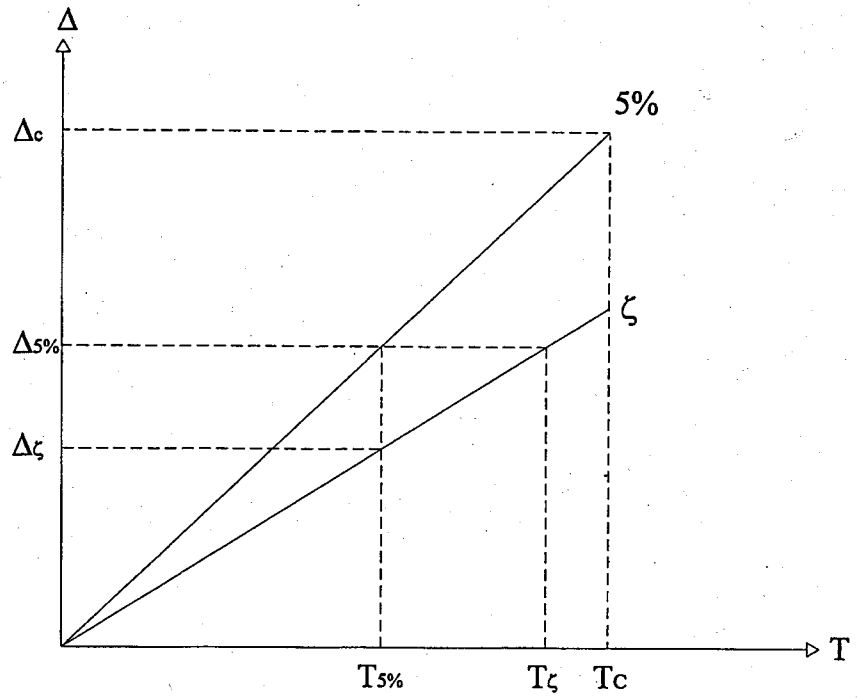

Figure 1.3. Displacement Response Spectrum for 5 per cent and ζ damping

As can be seen from Figure 1.3:

$$T_{5\%} = \frac{T_c}{\Delta_c}\Delta_{5\%} \tag{1.10}$$

$$T_\zeta = \frac{T_{5\%}}{\Delta_\zeta}\Delta_{5\%} \tag{1.11}$$

By putting (1.10) into (1.11),

$$T_\zeta = \frac{T_c}{\Delta_c \Delta_\zeta}\Delta_{5\%}^2 \tag{1.12}$$

Since Δ_ζ is defined in (1.9), by putting (1.9) into (1.12), period at ζ damping is readily obtained.

$$T_\zeta = \frac{T_c}{\Delta_c}\Delta_{5\%}\left(\frac{2+\zeta}{7}\right)^{1/2} \tag{1.13}$$

Once, effective period is found considering effective damping of the building, effective stiffness can be expressed by (1.14) from consideration of a SDOF oscillator where the variable m_{eff} represents the effective mass and is given by (1.15).

$$K_{eff} = \frac{4\pi^2}{T_\zeta^2} m_{eff} \tag{1.14}$$

$$m_{eff} = \sum_{i=1}^{ns} \frac{\Delta_i}{\Delta_{5\%}} m_i \tag{1.15}$$

Effective stiffness can be further expressed by putting (1.13) into (1.14) where target displacement is calculated from Equation (1.17)

$$K_{eff} = \frac{4\pi^2 m_{eff}}{\Delta_{5\%}^2}\frac{\Delta_c^2}{T_c^2}\left(\frac{7}{2+\zeta}\right) \tag{1.16}$$

$$\Delta_{5\%} = \frac{\sum_{i=1}^{ns} m_i \Delta_i^2}{\sum_{i=1}^{ns} m_i \Delta_i} \tag{1.17}$$

Base shear is simply the product of effective stiffness and target displacement, so by multiplying (1.16) and (1.17) base shear is readily obtained.

$$V_b = \frac{4\pi^2 m_{eff}}{\Delta_{5\%}}\frac{\Delta_c^2}{T_c^2}\left(\frac{7}{2+\zeta}\right) \tag{1.18}$$

2. TARGET DISPLACEMENT PROFILE METHOD

2.1. General

The determination of the target displacement profile is the core part of direct displacement based design since, when the structure achieves to specified target displacement under earthquake demand, it should be provided that the global response of the structure and the individual component deformations do not exceed specific performance limits for the building.

In the case of cantilever structural walls, constructing a mathematical model to assign a target displacement profile is rather easy as compared to frame systems for; each of the cantilever structural walls has only one potential plastic hinge that is readily known to be at the base. In this chapter, a pre introduced mathematical model by Kowalsky [5] is studied. σ

2.2. Kowalski's Mathematical Model for Target Displacement Profile

Kowalski's mathematical model for determining target displacement profile is based on the UBC drift limit of $\theta_{lim} = 0.02$ or 0.025 depending on the fundamental period of building. As stated in ATC 40 [7], for life safety the maximum total drift limit of 0.02 is recommended because significant experience with responses to larger deformation levels is lacking. Laboratory tests on relatively complete structural systems seldom extend beyond this deformation level. Furthermore, most tests have been conducted on structures satisfying or nearly satisfying current proportioning and detailing requirements for new buildings. Measured responses of buildings subjected to actual earthquakes also do not extent beyond this limit. The displacement profile, Δ_i, is obtained by (2.1) where Δ_{ei} is the elastic profile and Δ_{pi} is the plastic profile.

$$\Delta_i = \Delta_{ei} + \Delta_{pi} \tag{2.1}$$

2.2.1 Elastic Displacement Profile

When calculating elastic displacement profile it is assumed that yield curvature ϕ_y will coincide with the first yield of tensile reinforcement. The actual curvature distribution at yield will be nonlinear as a result of the basic nonlinear moment curvature relationship and because of local tension stiffening between cracks [7]. However, linear approximation is adopted as shown in Figure 2.1(c).

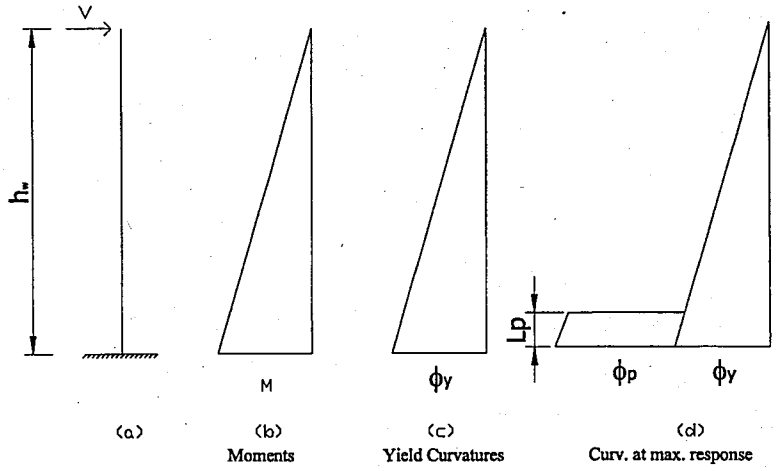

Figure 2.1. Moment and curvature relationships for reinforced concrete cantilever

Elastic rotation can be calculated by integrating yield curvature along the height.

$$\theta_e = \int_{h_i} \phi_y \frac{(h_w - h_i)}{h_w} dh_i \tag{2.2}$$

$$\theta_e = \int_{h_i} \phi_y dh_i + \int_{h_i} \phi_y \frac{h_i}{h_w} dh_i \tag{2.3}$$

$$\theta_e = \phi_y h_i - \frac{\phi_y h_i^2}{2h_w} \tag{2.4}$$

Again by integrating elastic rotation along the height, elastic displacement profile is readily obtained as a function of wall height as shown in (2.5).

$$\Delta_e = \int_{h_i} \theta_e = \int_{h_i} \phi_y h_i dh_i - \int_{h_i} \frac{\phi_y h_i^2}{2h_w} dh_i \tag{2.5}$$

$$\Delta_e = \frac{\phi_y h_i^2}{2} - \frac{\phi_y h_i^3}{6h_w} \tag{2.6}$$

By rearranging Equation (2.6), elastic displacement profile can be expressed as:

$$\Delta_e = \frac{\phi_y h_i^2}{3}(1.5 - \frac{h_i}{2h_w}) \tag{2.7}$$

2.2.2. Plastic Displacement Profile

As can be seen from Figure 2.1(d), it is idealized that plastic curvature is accumulated at an equivalent plastic hinge length L_p. The length L_p is chosen such that the plastic displacement at the top of the cantilever Δ_p, predicted by the simplified approach is the same as that derived from the actual curvature distribution. Assuming the plastic rotation to be concentrated at midheight of the plastic hinge, the plastic displacement profile is thus

$$\Delta_{pi} = (\theta_p)\left(h_i - \frac{L_p}{2}\right) \tag{2.8}$$

In Equation (2.8) plastic rotation θ_p is given by Equation (2.9) where θ_{et} is the top storey elastic rotation which is shown in Equation (2.10).

$$\theta_p = (\theta_{lim} - \theta_{et}) \tag{2.9}$$

$$\theta_{et} = \frac{\phi_y h_w}{2} \tag{2.10}$$

2.3. Target Displacement Profile of 150x20 Structural Wall

For wall height h_w = 12m, wall length l_w = 1.5m, longitudinal bar yield stress f_y = 420 Mpa and longitudinal bar diameter d_{bl} = 14mm, plastic hinge length L_p is calculated from greater of Equations (2.11) and (2.12)

$$L_p = 0.2x1.5 + 0.044\left(\frac{2}{3}x12\right) = 0.65m \tag{2.11}$$

$$L_p = 0.08\left(\frac{2}{3}x12\right) + 0.022x420x14/1000 = 0.77m \tag{2.12}$$

L_p is taken as 0.8m. Elastic modulus for longitudinal bar is 200,000 Mpa. So, longitudinal bar yield strain is:

$$\varepsilon_y = \frac{f_y}{E_s} = \frac{420}{200000} = 2.1E^{-3} \tag{2.13}$$

By assuming that the neutral axis depth is the half of the wall length, yield curvature is found by (2.14)

$$\phi_y = 2\epsilon_y / l_w = 2x2.1E^{-3}/1.5 = 2.8\,E^{-3}\ 1/m \tag{2.14}$$

Elastic displacement profile is then obtained by (2.15)

$$\theta_e = \phi_y h_i - \frac{\phi_y h_i^2}{2h_w} \tag{2.15}$$

For $h_1 = 3m$, $\Delta_{e1} = 0{,}012m$

For $h_2 = 6m$, $\Delta_{e2} = 0{,}042m$

For $h_3 = 9m$, $\Delta_{e3} = 0{,}085m$

For $h_4 = 12m$, $\Delta_{e4} = 0{,}134m$

Elastic rotation at top-storey θ_{et} is calculated by (2.16)

$$\theta_{et} = \frac{\phi_y h_w}{2} = \frac{2.8E^{-3}12}{2} = 0.017rad \tag{2.16}$$

By taking rotational limit $\theta_{lim} = 0.02$, plastic displacement profile is readily obtained by (2.17)

$$\Delta_{pi} = (\theta_{lim} - \theta_{et})\left(h_i - \frac{L_p}{2}\right) \tag{2.17}$$

For $h_1 = 3m$, $\Delta_{p1} = 0{,}008m$

For $h_2 = 6m$, $\Delta_{p2} = 0{,}018m$

For $h_3 = 9m$, $\Delta_{p3} = 0{,}028m$

For $h_4 = 12m$, $\Delta_{p4} = 0{,}037m$

The target displacement profile is given in (2.18)

$$\Delta_i = \Delta_{ei} + \Delta_{pi} \tag{2.18}$$

Thus, target displacement profile is calculated as:

For $h_1 = 3m$, $\Delta_1 = 0{,}020m$

For $h_2 = 6m$, $\Delta_2 = 0{,}060m$

For $h_3 = 9m$, $\Delta_3 = 0{,}113m$

For $h_4 = 12m$, $\Delta_4 = 0{,}172m$

2.4. Target Displacement Profile of 300x20 Structural Wall

For wall height h_w = 12m, wall length l_w = 3 m, longitudinal bar yield stress f_y = 420 Mpa and longitudinal bar diameter d_{bl} = 14mm.

$$L_p = 0.2x3 + 0.044\left(\frac{2}{3}x12\right) = 9.52m \tag{2.19}$$

$$L_p = 0.08\left(\frac{2}{3}x12\right) + 0.022x420x14/1000 = 0.77m \tag{2.20}$$

L_p is taken as 1.0m. Elastic modulus for longitudinal bar is 200,000 Mpa. So, longitudinal bar yield strain is:

$$\varepsilon_y = \frac{f_y}{E_s} = \frac{420}{200000} = 2.1E^{-3} \tag{2.21}$$

By assuming that the neutral axis depth is the half of the wall length, yield curvature is found by (2.22)

$$\phi_y = 2\epsilon_y / l_w = 2x2.1E^{-3}/3 = 1.4\,E^{-3}\ 1/\text{m} \tag{2.22}$$

Elastic displacement profile is obtained by (2.23).

$$\theta_e = \phi_y h_i - \frac{\phi_y h_i^2}{2h_w} \tag{2.23}$$

For h_1 = 3m , Δ_{e1} = 0,006m

For h_2 = 6m , Δ_{e2} = 0,021m

For h_3 = 9m , Δ_{e3} = 0,043m

For h_4 = 12m , Δ_{e4} = 0,067m

Elastic rotation at top-storey θ_{et} is calculated by (2.24)

$$\theta_{et} = \frac{\phi_y h_w}{2} = \frac{1.4E^{-3}12}{2} = 0.008rad \tag{2.24}$$

By taking rotational limit θ_{lim} = 0.02, plastic displacement profile is readily obtained by (2.25).

$$\Delta_{pi} = (\theta_{\text{lim}} - \theta_{et})\left(h_i - \frac{L_p}{2}\right) \tag{2.25}$$

For h_1 = 3m , Δ_{p1} = 0,029m

For h_2 = 6m , Δ_{p2} = 0,064m

For h_3 = 9m , Δ_{p3} = 0,099m

For h_4 = 12m , Δ_{p4} = 0,133m

The target displacement profile is given in (2.26)

$$\Delta_i = \Delta_{ei} + \Delta_{pi} \tag{2.26}$$

Thus, target displacement profile is calculated as:

For h_1 = 3m , Δ_1 = 0,035m

For h_2 = 6m , Δ_2 = 0,085m

For h_3 = 9m , Δ_3 = 0,141m

For h_4 = 12m , Δ_4 = 0,201m

2.5. Comment on Mathematical Model for Target Displacement Profile

As can be seen from Figure 2.1(d), curvature at max response is the sum of plastic curvature and yield (elastic) curvature. So, total rotation within a specified length L_p can be described as the accumulation of maximum curvature along the plastic length which is idealized as:

$$\theta_t = (\phi_p + \phi_y) L_p \tag{2.27}$$

$$\theta_t = \theta_p + \theta_e \tag{2.27}$$

For the smaller values of θ_t as in the case it can be assumed that θ_t is equal to $\tan(\theta_t)$, which is the limit drift ratio θ_{lim} defined by Kowalsky. However Kowalsky formulized limit drift ratio as the sum of plastic rotation, and elastic rotation which is accumulated not within the plastic length but at the top storey.

As can be seen from Equation (2.10) top-storey elastic rotation is directly related with wall height, h_w. So, for the higher wall lengths this top-storey elastic rotation increases so that there is left limited or no room for plastic rotation within a specified drift limit. Therefore, mathematical model proposed for Kowalsky impose elastic design for higher wall lengths. For example if we consider a 150cm length structural wall, by assuming that the natural axis depth is the half of the wall length the yield curvature would be:

$$\phi_y = 2\epsilon_y / l_w \tag{2.28}$$

Elastic modulus for longitudinal bar is 200,000 Mpa. So, longitudinal bar yield strain is:

$$\varepsilon_y = \frac{f_y}{E_s} = \frac{420}{200000} = 2.1E^{-3} \tag{2.29}$$

Solving the Equation (2.28) yield curvature is found 2.8 E^{-3} 1/m. By rearranging Equation (2.10) and setting top-storey elastic rotation 0.02 which is the limit drift ratio, then ultimate wall height satisfying the drift criteria is given by Equation (2.30).

$$h_w = \frac{2\theta_{et}}{\phi_y} = \frac{0.02 * 2}{2.8E^{-3}} = 14m \tag{2.30}$$

For the average storey height of 3m, this means one could not design a building more than 4 stories when 150cm length structural walls are used even if it is an elastic design and no matter how stiff the building is.

The ductility ratio of the 150x20 structural wall is only 1.28, which means its expected behavior under seismic loading is nearly elastic. However, ductility ratio of the 300x20 structural wall is 2.99. This increase in ductility is due to decreased curvature and in turn decreased top-storey elastic rotation enabling some plastic rotation within a specified drift limit.

Also, output drift ratios don't match with target drift ratio specified at the beginning of the design. For 150x20 structural wall drift ratio is 0.014 and for 300x20 structural wall it is 0.017 however, design input was 0.020.

It is apparent that mathematical model proposed by Kowalsky needs a revision for it directs designer to unnecessary path of elastic design for slender structural wall configurations. This is direct contrast to our knowledge of taller buildings are less susceptible to seismic attack than shorter ones depending on their first natural vibration period.

3. REVISED TARGET DISPLACEMENT PROFILE

3.1. General

In this chapter a revised mathematical model is introduced to estimate target displacement profile. The requirement for a revised mathematical model was discussed in Chapter 2. Kowalsky's mathematical model is based on a drift ratio limit consisting of plastic rotation at plastic zone and elastic rotation at top storey. Since elastic rotation at top storey is proportional to wall height, for higher wall heights it becomes so that there is left no room for plastic rotation to satisfy drift ratio limit, which in turn forces designer for an elastic design.

This chapter also covers a parametric study in which, cantilever structural walls with different sectional properties are modeled by equivalent columns and the accuracy of the model is checked with a more rigorous finite element model. For representation of nonlinear behavior of structural walls, predefined plastic zones are modeled with nonlinear link elements. Reinforced concrete material model is consisted of bilinear representation of moment-curvature relationship for structural wall.

Second phase of the parametric study involves a comparison between the design and analysis of the cantilever structural walls. Structural walls with different wall lengths are designed according to revised mathematical model and the compatibility of the results are reviewed with the ones of above defined model.

3.2. Revised Mathematical Model for Target Displacement Profile

In the mathematical model proposed by Kowalsky [5] UBC drift limit of 0.02 and 0.025 is used, depending on the fundamental period of vibration of the building. Since these drift ratios are so small they are assumed to be equal to max. rotation which is idealized to take place at midheight of the plastic hinge. However, plastic rotation, which is also assumed to be concentrated at midheight of the plastic hinge, is formalized by subtracting elastic rotation at top storey, θ_{et}, from limit drift ratio, θ_{lim}, or in other words

limit rotation. On the other hand, if we assume that the plastic curvature ϕ_p is equal to maximum plastic curvature ϕ_m - ϕ_y then plastic rotation is given by:

$$\theta_p = \phi_p L_p = (\phi_m - \phi_y) L_p \tag{3.1}$$

If we update the plastic rotation given in Equation (2.8) with Equation (3.1), the plastic displacement profile becomes:

$$\Delta_{pi} = (\phi_m - \phi_y) L_p \left(h_i - \frac{L_p}{2} \right) \tag{3.2}$$

By setting maximum rotation as limit rotation, and defining $\phi_y.L_p$ as elastic rotation at plastic hinge, θ_e, plastic displacement profile is thus

$$\Delta_{pi} = (\theta_{\text{lim}} - \theta_e) \left(h_i - \frac{L_p}{2} \right) \tag{3.3}$$

It should be noted that by defining plastic displacement profile as in Equation (3.3), the target displacement profile is no longer based on the limit drift ratios but the limit hinge rotations which are the main criteria together with the global drift ratios for assessing the calculated building response and defined by ATC 40 [7].

3.3. Structural Wall Modeling

The aspect ratio (height/length) of the structural walls exceeds 4, so they may be considered slender. Since, slender walls are generally controlled by flexural behavior the equivalent column model can be used. The analytical model represents a cantilever structural wall with an equivalent wide column element located at the wall centerline.

Two structural walls are modeled for parametric study purposes. One has section dimensions 150x20 with wall aspect ratio 8, and the other has section dimensions 300x20 with wall aspect ratio 4. As can be seen from Figure 3.1 different models are constructed

for each wall. Model (a) is the finite element model with mesh sizes 50x50; model (b) is the equivalent column model and model (c) is the enhanced equivalent column model in which a plastic nonlinear link element is located at the plastic zone to account for the nonlinear behavior of structural wall.

Nonlinear analysis capabilities are available through a nonlinear link element (NLLink). Uniaxial plasticity type of nonlinear behavior is modeled with the link element. Each element is assumed to be composed of three separate nonlinear springs, one for each of the three deformational degrees-of freedom which are U1, U2 and R3. U1 and U2 are the degrees-of freedom parallel to global X and global Z axes respectively and their effective stiffness is given by (3.4) where E is the modulus of elasticity for reinforced concrete, I is the moment of inertia and L_p is the length of NLLink element. R3 is the rotational degree-of freedom around global Y axis and its effective stiffness is given by (3.5). The force-deformation relationships of these springs are independent of each other.

$$U_1 = U_2 = \frac{12EI}{L_p^3} \tag{3.4}$$

$$R_3 = \frac{EI}{L_p} \tag{3.5}$$

For V = 100KN, E = 30000 Mpa and L_p = 0.8 m the results are given in Table 3.1.

The analysis model for a structural wall element should represent the strength, stiffness, and deformation capacity of the wall for in-plane loading. It can be seen from Table 3.1 that as far as the scope of this thesis is concerned, enhanced equivalent column model is acceptable for modeling structural walls. With respect to finite element model the error in top displacement is only 1.57 per cent for aspect ratio 8 and the error is 1.58 per cent for aspect ratio 4. So, throughout this thesis enhanced equivalent column model is used for modeling purposes.

1- MODELS FOR 150X20 STRUCTURAL WALL

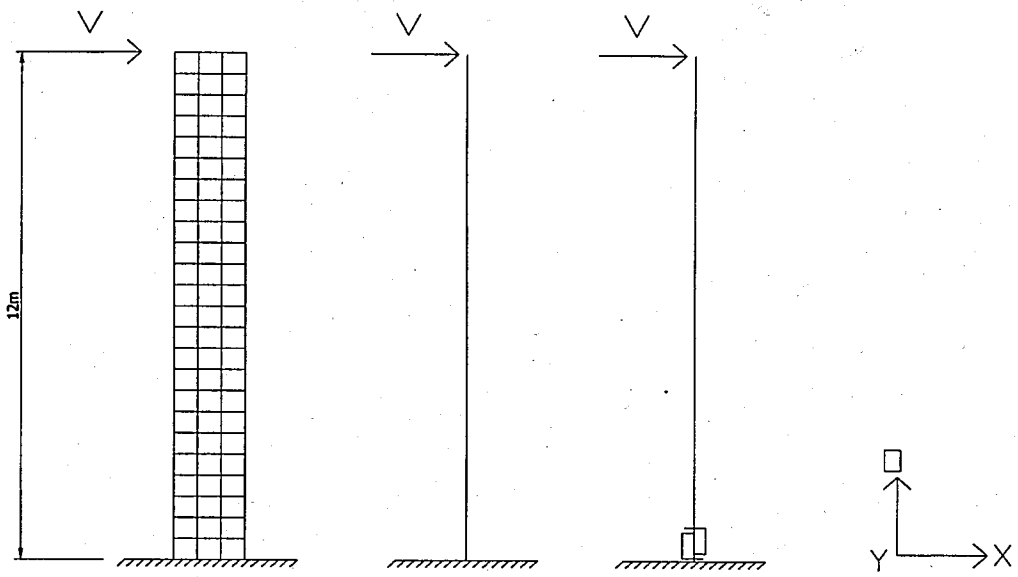

a-) Finite Element Model b-) Equivalent Column Model c-) Enhanced Equivalent Column Model

2- MODELS FOR 300X20 STRUCTURAL WALL

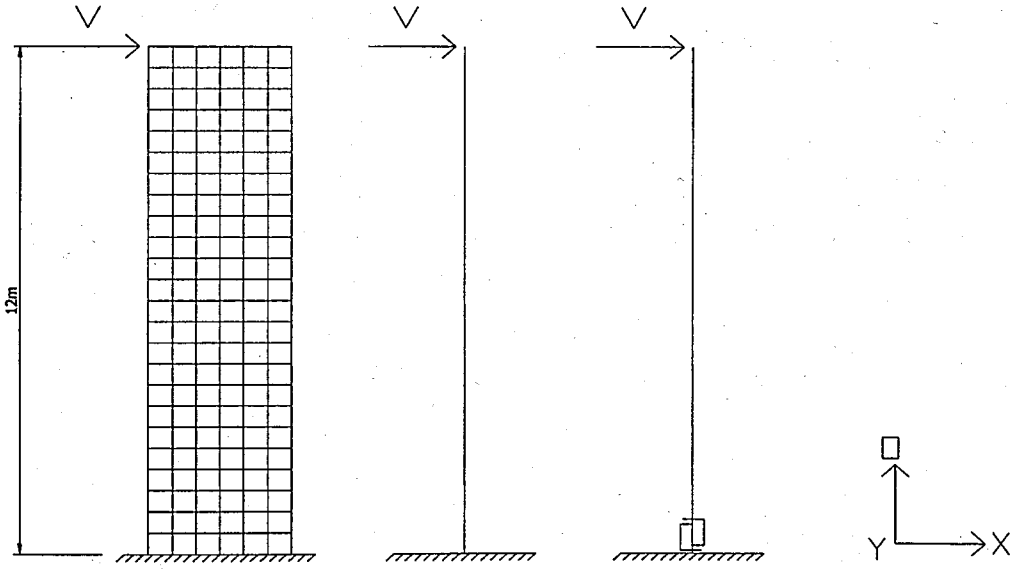

a-) Finite Element Model b-) Equivalent Column Model c-) Enhanced Equivalent Column Model

Figure 3.1. Structural wall models

Table 3.1. Comparison table for Model 1 and Model 2

		Description of Model	Top Displacement (m)	Base Moment (KNm)
Model 1	a	Finite Element Model for 150x20 Structural Wall	0.3440	12000
	b	Equivalent Column Model for 150x20 Structural Wall	0.3452	12000
	c	Enhanced Equivalent Column Model for 150x20 Structural Wall	0.3494	12000
Model 2	a	Finite Element Model for 300x20 Structural Wall	0.0443	12000
	b	Equivalent Column Model for 300x20 Structural Wall	0.0446	12000
	c	Enhanced Equivalent Column Model for 300x20 Structural Wall	0.0450	12000

3.4. Plastic Hinge Rotations

3.4.1. Design Target Displacement Profile of 150x20 Structural Wall

First step in obtaining target displacement profile is the determination of plastic hinge length L_p. For wall height h_w = 12m, wall length l_w = 1.5m, longitudinal bar yield stress f_y = 420 Mpa and longitudinal bar diameter d_{bl} = 14mm.

$$L_p = 0.2x1.5 + 0.044\left(\frac{2}{3}x12\right) = 0.65m \tag{3.6}$$

$$L_p = 0.08\left(\frac{2}{3}x12\right) + 0.022x420x14/1000 = 0.77m \tag{3.7}$$

L_p is taken as 0.8m. Elastic modulus for longitudinal bar is 200,000 Mpa. So, longitudinal bar yield strain is:

$$\varepsilon_y = \frac{f_y}{E_s} = \frac{420}{200000} = 2.1E^{-3} \tag{3.8}$$

By assuming that the neutral axis depth is the half of the wall length, yield curvature is found by (3.9)

$$\phi_y = 2\epsilon_y / l_w = 2\text{x}2.1E^{-3}/1.5 = 2.8\,E^{-3}\ 1/\text{m} \tag{3.9}$$

Elastic displacement profile is then obtained by (3.10)

$$\theta_e = \phi_y h_i - \frac{\phi_y h_i^2}{2h_w} \tag{3.10}$$

For h_1 = 3m , Δ_{e1} = 0,012m

For h_2 = 6m , Δ_{e2} = 0,042m

For h_3 = 9m , Δ_{e3} = 0,085m

For h_4 = 12m , Δ_{e4} = 0,134m

Elastic rotation at plastic hinge θ_e is calculated by (3.11)

$$\theta_e = \phi_y L_p = 2.8E^{-3}x0.8 = 2.24E^{-3}rad \tag{3.11}$$

By taking rotational limit θ_{lim} = 0.02, plastic displacement profile is readily obtained by (3.12)

$$\Delta_{pi} = (\theta_{\text{lim}} - \theta_e)\left(h_i - \frac{L_p}{2}\right) \tag{3.12}$$

For h_1 = 3m , Δ_{p1} = 0,046m

For h_2 = 6m , Δ_{p2} = 0,099m

For h_3 = 9m , Δ_{p3} = 0,153m

For h_4 = 12m , Δ_{p4} = 0,206m

The target displacement profile is given in (3.13)

$$\Delta_i=\Delta_{ei}+\Delta_{pi} \tag{3.13}$$

Thus, target displacement profile is calculated as:

For $h_1 = 3m$, $\Delta_1 = 0{,}058m$

For $h_2 = 6m$, $\Delta_2 = 0{,}141m$

For $h_3 = 9m$, $\Delta_3 = 0{,}238m$

For $h_4 = 12m$, $\Delta_4 = 0{,}340m$

3.4.2. Design Target Displacement Profile of 300x20 Structural Wall

For wall height h_w = 12m, wall length l_w = 3 m, longitudinal bar yield stress f_y = 420 Mpa and longitudinal bar diameter d_{bl} = 14mm.

$$L_p = 0.2x3 + 0.044\left(\frac{2}{3}x12\right) = 9.52m \tag{3.14}$$

$$L_p = 0.08\left(\frac{2}{3}x12\right) + 0.022x420x14/1000 = 0.77m \tag{3.15}$$

L_p is taken as 1.0m. Elastic modulus for longitudinal bar is 200,000 Mpa. So, longitudinal bar yield strain is:

$$\varepsilon_y = \frac{f_y}{E_s} = \frac{420}{200000} = 2.1E^{-3} \tag{3.16}$$

By assuming that the neutral axis depth is the half of the wall length, yield curvature is found by (3.17)

$$\phi_y = 2\epsilon_y / l_w = 2x2.1E^{-3}/3 = 1.4\,E^{-3}\ 1/m \tag{3.17}$$

Elastic displacement profile is obtained by (3.18).

$$\theta_e = \phi_y h_i - \frac{\phi_y h_i^2}{2h_w} \tag{3.18}$$

For $h_1 =$ 3m , $\Delta_{e1} = 0{,}006m$

For $h_2 =$ 6m , $\Delta_{e2} = 0{,}021m$

For $h_3 =$ 9m , $\Delta_{e3} = 0{,}043m$

For $h_4 =$ 12m , $\Delta_{e4} = 0{,}067m$

Elastic rotation at plastic hinge θ_e is calculated by (3.19)

$$\theta_e = \phi_y L_p = 1.4E^{-3}x1.0 = 1.40E^{-3}rad \tag{3.19}$$

By taking rotational limit θ_{lim} = 0.02, plastic displacement profile is readily obtained by (3.20).

$$\Delta_{pi} = (\theta_{lim} - \theta_e)\left(h_i - \frac{L_p}{2}\right) \tag{3.20}$$

For $h_1 =$ 3m , $\Delta_{p1} = 0{,}047m$

For $h_2 =$ 6m , $\Delta_{p2} = 0{,}102m$

For $h_3 =$ 9m , $\Delta_{p3} = 0{,}158m$

For $h_4 =$ 12m , $\Delta_{p4} = 0{,}214m$

The target displacement profile is given in (3.21)

$$\Delta_i = \Delta_{ei} + \Delta_{pi} \tag{3.21}$$

Thus, target displacement profile is calculated as:

For $h_1 = 3m$, $\Delta_1 = 0{,}052m$

For $h_2 = 6m$, $\Delta_2 = 0{,}123m$

For $h_3 = 9m$, $\Delta_3 = 0{,}201m$

For $h_4 = 12m$, $\Delta_4 = 0{,}281m$

3.4.3. Analysis

In order to check the accuracy of the target displacement profiles which are obtained for cantilever structural walls having section dimensions 150x20 and 300x20, a series of moment-curvature analyses are conducted for the sections defined in Table 3.2. To inspect the effect of reinforcement content, both of the sections have designed with minimum and maximum reinforcement. Concrete compression strength is selected as 25 Mpa, while longitudinal bar yield stress is selected as 420 Mpa. Longitudinal bars are of 14mm in diameter.

Table 3.2. Section details of structural walls

Section Definition	Boundary Zone Bars	Boundary Zone Bar Size	Per cent Longitudinal Steel
150x20(min rein)	6	14	0.83%
150x20(max rein)	12	14	1.44%
300x20(min rein)	6	14	0.49%
300x20(max rein)	12	14	0.80%

Results of moment-curvature analyses are shown in Figures 3.2 and 3.3. To calculate EI effective and effective yield moment, the nonlinear moment-curvature is idealized providing that the area below the nonlinear curve and the bilinear curve is approximately equal to each other. Results are shown in Table 3.3.

Once the moment-curvature analysis results are obtained, cantilever structural walls can be modeled as defined in Section 3.2. The EI effective values are divided by Modulus of Elasticity which is 30,000,000 KN/m2 for C25 Concrete. The moment of inertia obtained is the effective moment of inertia I_{eff} and it is a fraction of gross section moment of inertia I_g. So, a modification factor is calculated by (3.21) for each of the sections and the stiffness characteristics of the model are modified accordingly.

$$MF = \frac{I_{eff}}{I_g} \tag{3.21}$$

Table 3.3. Moment-Curvature analysis results

Section Definition	EI Effective KN-m2	Yield EI Effective KN-m2	Effective Yield Moment KN	Ultimate Moment KN	Effective Yield Curvature 1/m
150x20(min rein)	2.93E+05	9.42E+02	707	792	0.00241
150x20(max rein)	4.89E+05	1.33E+03	1200	1330	0.00245
300x20(min rein)	1.41E+06	4.28E+03	1761	1948	0.00125
300x20(max rein)	2.30E+06	5.55E+03	2800	3052	0.00122

The pre yield and post yield modification factors as well as the calculated directional stiffness values for NLLink elements are shown in Tables 3.4 and 3.5 respectively

When the model is constructed for each of the sections, it is pushed until the base moment reaches to effective yield moment. At that point, displacement values for each of the storey is read and noted as elastic displacements. Also the rotations at NLLink elements are noted as elastic rotations. For the post yield stage directional properties of the NLLink elements are modified with the ones in Table 3.5 and the system is further pushed until the total top displacements coincide with the ones of design. Total displacement profile and the total rotations at NLLink elements are noted. The results are given in Tables 3.6 and 3.7.

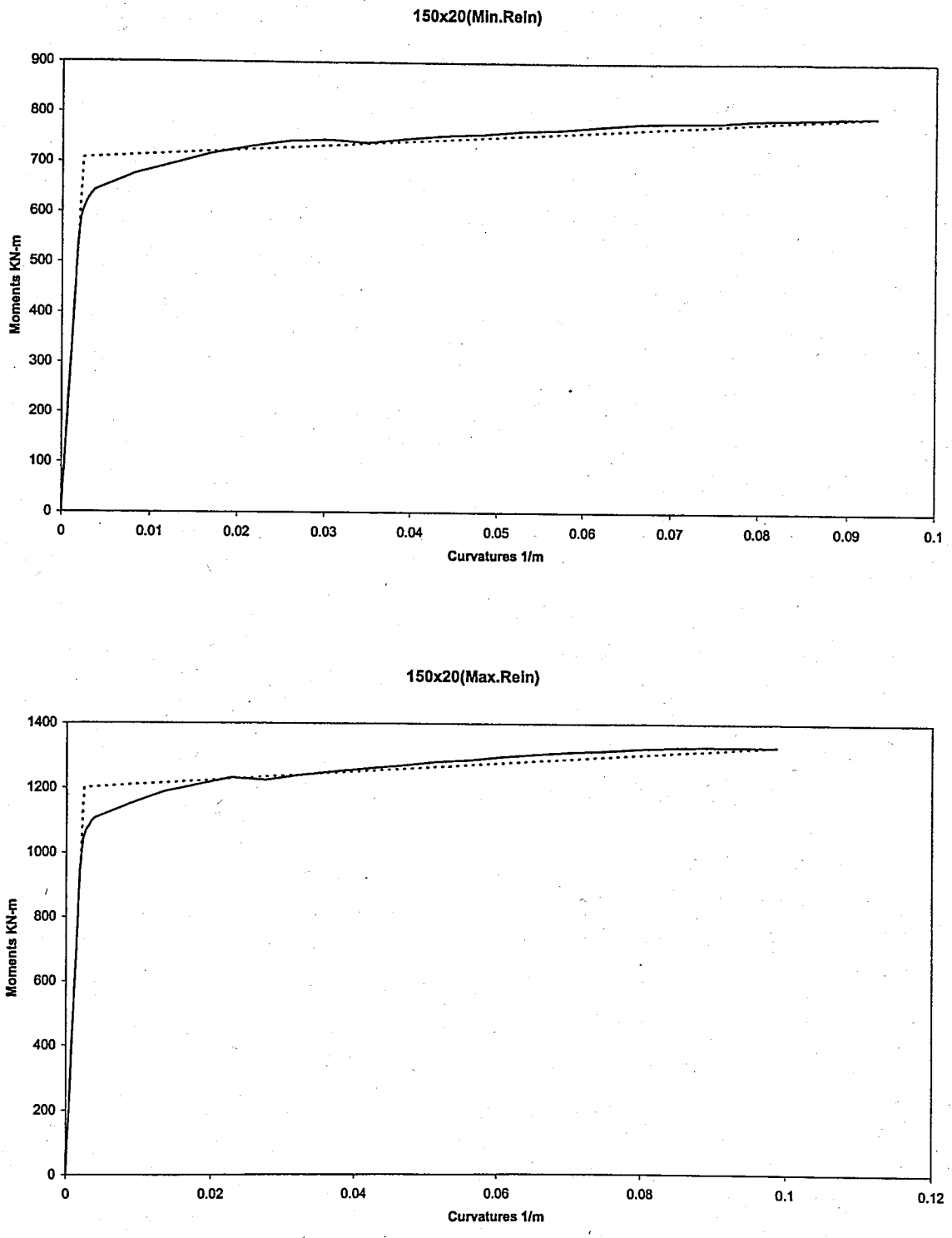

Figure 3.2. Moment-Curvature relationships for section 150x20

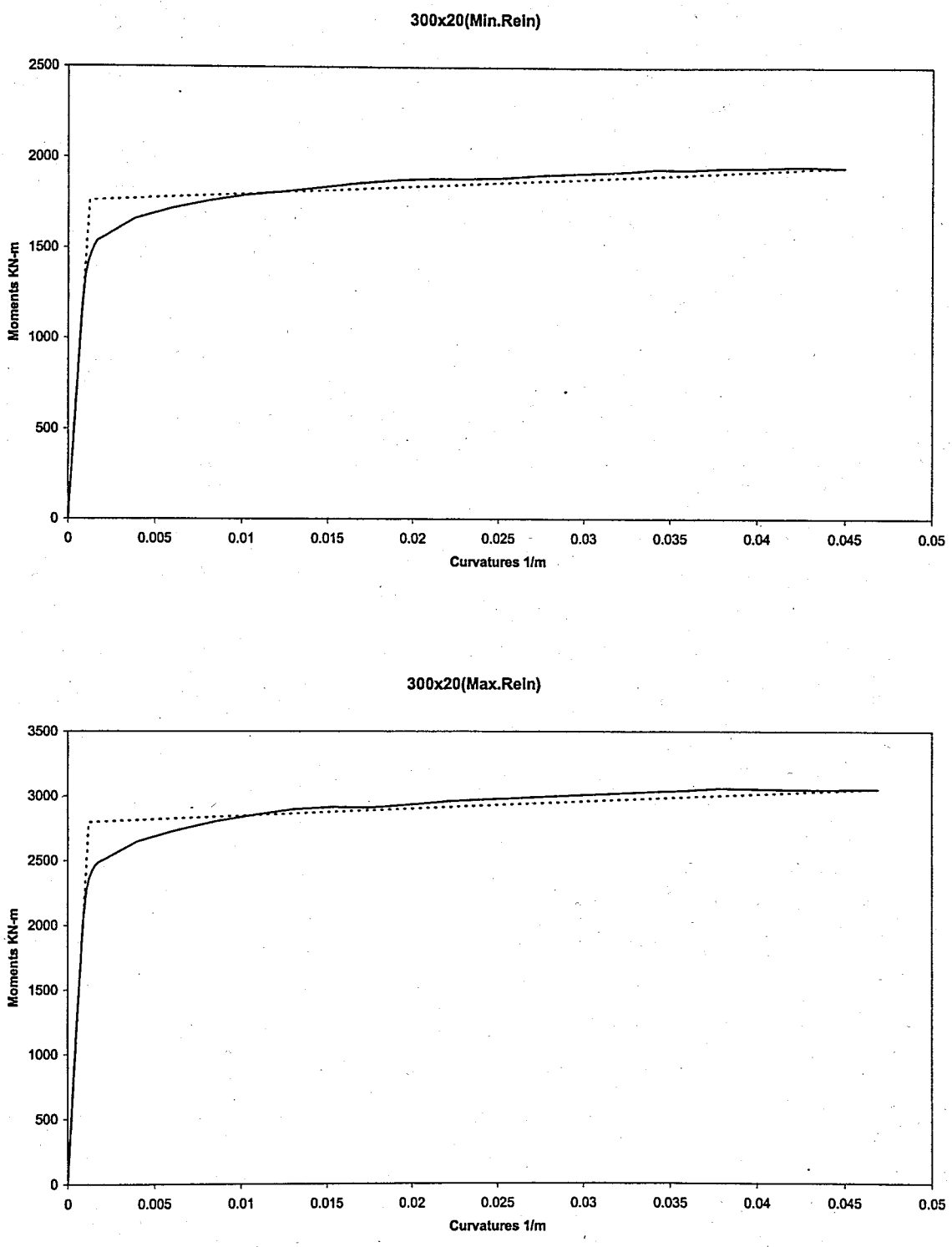

Figure 3.3. Moment-Curvature relationships for section 300x20

Table 3.4. Pre yield modification factors and NLLink directional properties

	EI Effective KN-m2	I Effective m4	Ig m4	M.F.	R3 KN-m	U2 KN/m
150x20(min rein)	2.93E+05	9.77E-03	5.63E-02	0.1736	3.66E+05	6.87E+06
150x20(max rein)	4.89E+05	1.63E-02	5.63E-02	0.2898	6.11E+05	1.15E+07
300x20(min rein)	1.41E+06	4.70E-02	4.50E-01	0.1044	1.41E+06	1.69E+07
300x20(max rein)	2.30E+06	7.67E-02	4.50E-01	0.1704	2.30E+06	2.76E+07

Table 3.5. Post yield modification factors and NLLink directional properties

	EI Effective KN-m2	I Effective m4	Ig m4	M.F.	R3 KN-m	U2 KN/m
150x20(min rein)	9.42E+02	3.14E-05	5.63E-02	0.0006	1.18E+03	2.21E+04
150x20(max rein)	1.33E+03	4.43E-05	5.63E-02	0.0008	1.66E+03	3.12E+04
300x20(min rein)	4.28E+03	1.43E-04	4.50E-01	0.0003	4.28E+03	5.14E+04
300x20(max rein)	5.55E+03	1.85E-04	4.50E-01	0.0004	5.55E+03	6.66E+04

3.4.4. Conclusion

As can be seen from Tables 3.6 and 3.7 analysis and design results are in conformity and it can be concluded that the mathematical model for assessing the target displacement profile is satisfactory. Although yield moments vary with different reinforcement content, the difference in modification factors and NLLink directional properties altered the situation so that reinforcement content does not affect the ultimate results in terms of total displacement profile and total rotation. Another important factor is, reinforcement content has very limited effect on yield curvature, and on the other hand the variation in section dimensions has some effect on yield curvature in terms of deviation from design. For section 300x20 the deviation from design is 12 per cent however, the deviation is 17 per cent for section 150x20. This means for squat walls design estimation for yield curvature is more accurate than that of the slender walls.

		DESIGN			150x20(min rein)			150x20(max rein)		
		ELASTIC	INELASTIC	TOTAL	ELASTIC	INELASTIC	TOTAL	ELASTIC	INELASTIC	TOTAL
DISPLACEMENT PROFILE (m)	S4	0,134	0,206	0,340	0,113	0,227	0,340	0,115	0,225	0,340
	S3	0,085	0,153	0,238	0,071	0,170	0,241	0,072	0,168	0,240
	S2	0,042	0,099	0,141	0,035	0,113	0,148	0,036	0,112	0,148
	S1	0,012	0,046	0,058	0,010	0,056	0,066	0,010	0,056	0,066
YIELD MOMENT (KNm)					707			1201		
YIELD CURV. (1/m)		0,0028			0,0024			0,0024		
DUCTILITY RATIO		2,53			3,01			2,96		
ROTATION		**0,020**			0,0019	0,0188	**0,021**	0,002	0,0186	**0,021**

Table 3.6. Comparison table between design and analysis of 150x20 structural wall

		DESIGN			300x20(min rein)			300x20(max rein)		
		ELASTIC	INELASTIC	TOTAL	ELASTIC	INELASTIC	TOTAL	ELASTIC	INELASTIC	TOTAL
DISPLACEMENT PROFILE (m)	S4	0,067	0,219	0,286	0,058	0,228	0,286	0,057	0,229	0,286
	S3	0,043	0,162	0,205	0,037	0,171	0,208	0,036	0,171	0,207
	S2	0,021	0,106	0,127	0,018	0,113	0,131	0,018	0,114	0,132
	S1	0,006	0,049	0,055	0,005	0,057	0,062	0,005	0,057	0,062
YIELD MOMENT (KNm)					1761			2799		
YIELD CURV. (1/m)		0,00140			0,00125			0,00122		
DUCTILITY RATIO		4,3			4,9			5,0		
ROTATION		**0,020**			0,001	0,0189	**0,020**	0,001	0,019	**0,020**

Table 3.7. Comparison table between design and analysis of 300x20 structural wall

3.5. Comparison of Original and Revised Target Displacement Profiles

Graphical representation of the target displacement profiles calculated according to original mathematical model and revised mathematical model is demonstrated in Figure 3.4. Disagreement in terms of top storey displacement is considerable especially for the slender walls. Also an important note is, according to revised mathematical model top-storey displacement is decreased with the increase in length of structural wall. This is as it should be due to stiffness change; however original model gives results on the contrary. The deformation level of 300cm length structural wall is higher than that of the 150cm length structural wall. This anomaly is due to the elastic design in slender walls as discussed in Chapter 2.

Also base shears are calculated according to procedure stated in Chapter 1. 100 ton mass is assumed to be lumped at each storey level. By taking each storey 3 m tall four stories are considered to maintain conformity with pre-calculated target displacement profiles. The results are stated in Figure 3.5. In the original model design base shear of the 150cm length wall is nearly twice of the 300cm length wall. It is again because of the elastic design in slender walls.

It is important to note that base shear is almost not affected from wall aspect ratio in revised mathematical model. This is due to combined effect of decreased deformation demand and increased ductility demand in higher wall lengths. Increase in ductility demand is because of the reduced elastic curvature in squat walls. So, reduced elastic rotation gives room to more plastic rotation within a specified rotation limit. Hence, this increase in ductility and effective damping give rise to additional energy dissipation change in seismic demand due to stiffness change. This effect is not captured in code-based design procedure and as a result of constant force reduction elastic base shear is reduced with decreased stiffness.

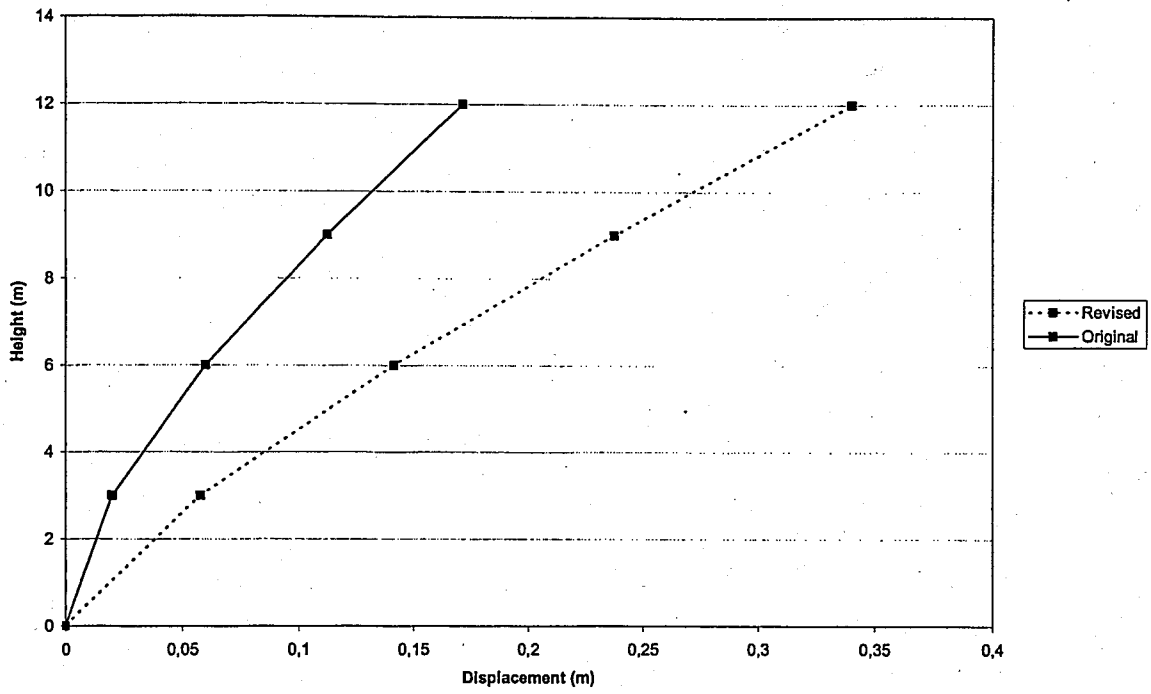

(a)

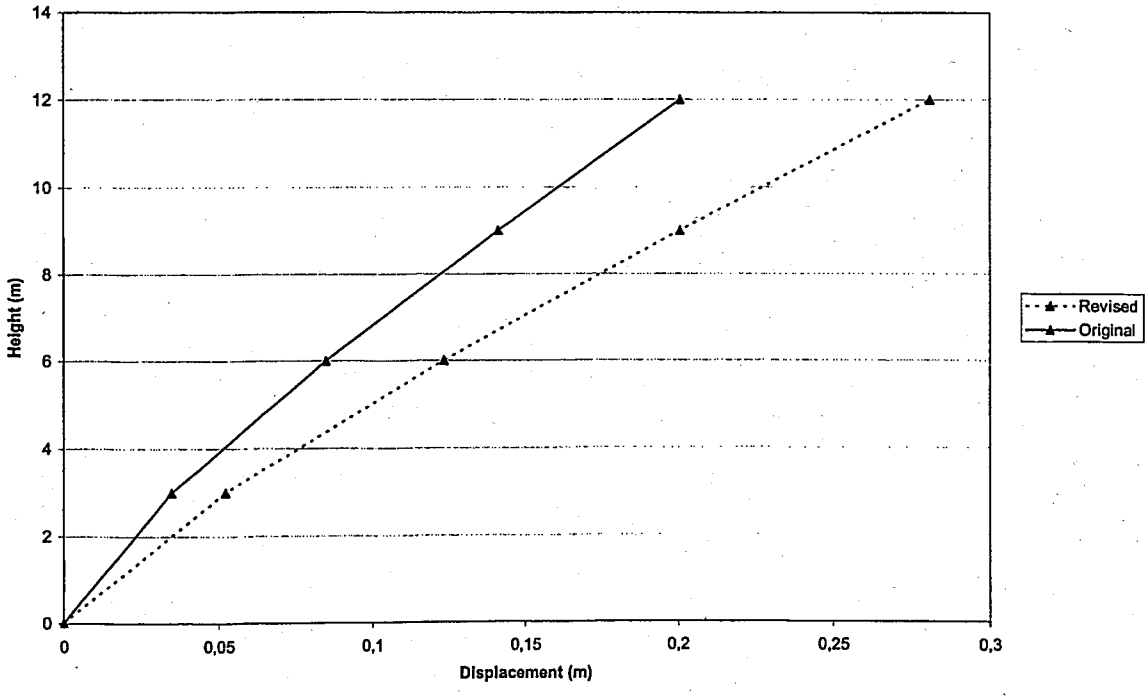

(b)

Figure 3.4. Target displacement profiles: (a) 150cm length structural wall; (b) 300cm length structural wall

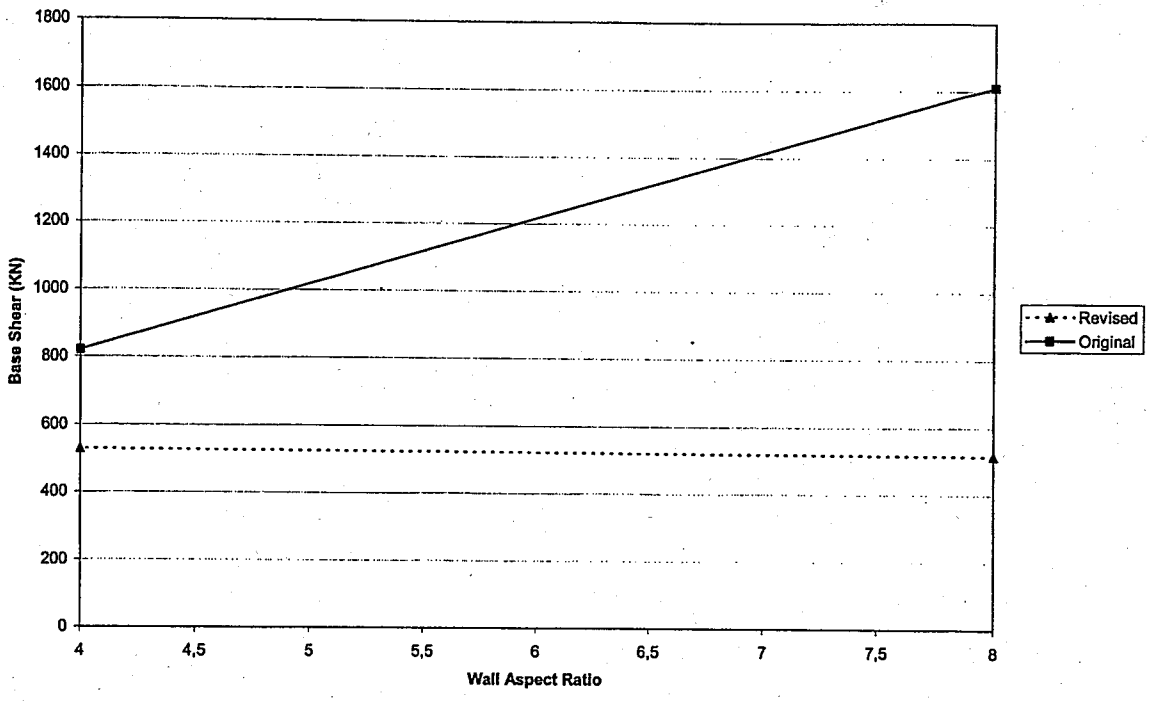

Figure 3.5. Base shear comaprison

4. REVISED EFFECTIVE DAMPING

4.1. Kowalsky Effective Damping

The damping relationship is derived considering the effect of ductility on damping and is related to the hysteretic energy absorbed. The relation is given in (4.1) and it is based on the Takeda [2] hysteretic model, Figure 4.1, for an unloading stiffness factor of n=0.5 and a bilinear stiffness ratio of r=0.05. It also includes an additive term of 5 per cent viscous damping.

$$\beta_{eff} = 100\left(0.05 + \frac{1 - \frac{0.95}{\sqrt{\mu_\Delta}} - 0.05\sqrt{\mu_\Delta}}{\pi}\right) \tag{4.1}$$

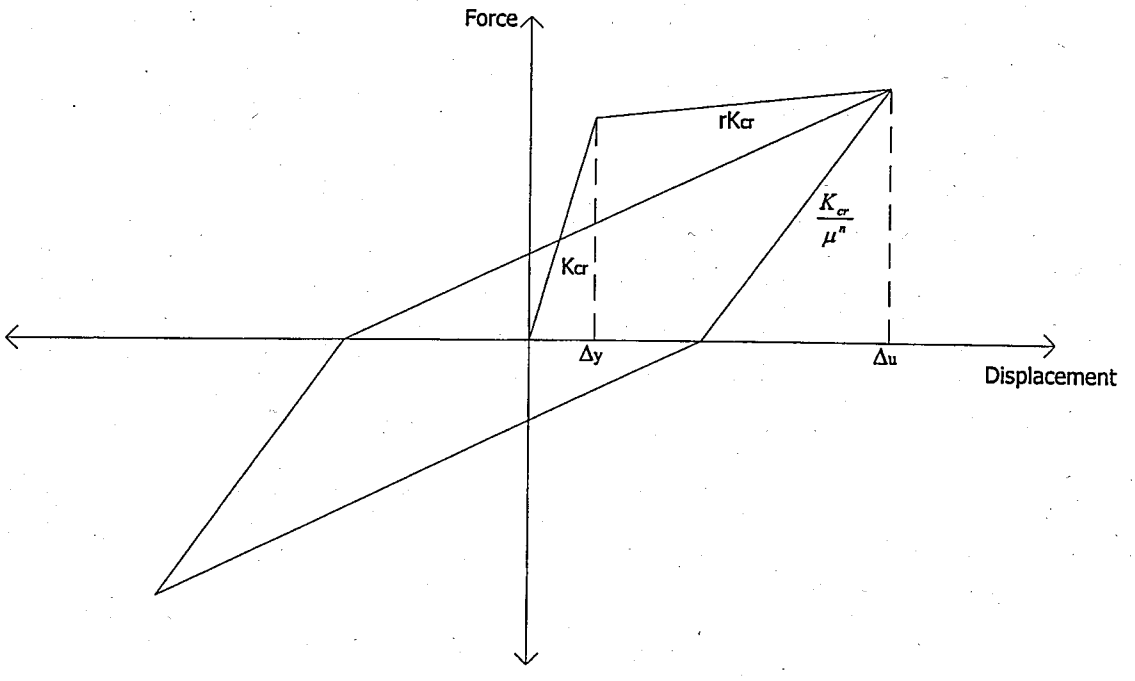

Figure 4.1. Takeda degrading stiffness hysteresis

4.2. ATC 40 Effective Damping

The damping that occurs when earthquake ground motion drives a structure into the inelastic range can be viewed as a combination of viscous damping that is inherent in the structure and hysteretic damping. Hysteretic damping is related to the area inside the loops that are formed when the base shear is plotted against the structure displacement. Hysteretic damping can be represented as equivalent viscous damping.

The equivalent viscous damping, β_{eq}, associated with a maximum displacement of d_{pi}, can be estimated from the following Equation where, β_o is the hysteretic damping represented as equivalent viscous damping and the term 0.05 represents 5 per cent viscous damping inherent in the structure (assumed to be constant).

$$\beta_{eq} = \beta_o + 0.05 \tag{4.2}$$

Hysteretic damping, β_o, can be calculated as:

$$\beta_o = \frac{1}{4\pi}\frac{E_D}{E_{So}} \tag{4.3}$$

Where, E_D is the energy dissipated by damping and E_{So} is the maximum strain energy. The physical significance of the terms E_D and E_{So} in Equation (4.3) is illustrated in Figure 4.2. E_D is the energy dissipated by the structure in a single cycle of motion, that is, the area enclosed by a single hysteresis loop. E_{So} is the maximum strain energy associated with that cycle of motion, that is, the area of hatched triangle.

To enable simulation of imperfect hysteresis loops (loops reduced in area), the concept of effective viscous damping using a damping modification factor, κ, has been introduced by ATC 40 [7] . Effective viscous damping, β_{eff}, is defined by:

$$\beta_{eff} = \kappa\beta_o + 5 \tag{4.4}$$

The κ-factor is a measure of the extent to which the actual building hysteresis is well represented by the parallelogram of Figure 4.2, either initially or after degradation. The κ-factor depends on the structure behavior of the building, which in turn depends on the quality of the seismic resisting system and the duration of ground shaking. Structural behavior Type A represents stable, reasonably full hysteresis loops most similar to Figure 4.2, and assigned a κ of 1.0 (except at higher damping values). Type B is assigned a basic κ of 2/3 and represents a moderate reduction of area (κ is also reduced at higher values of β_{eff}). Type C represents poor hysteretic behavior with a substantial reduction of loop area (severely pinched) and is assigned a κ of 1/3.

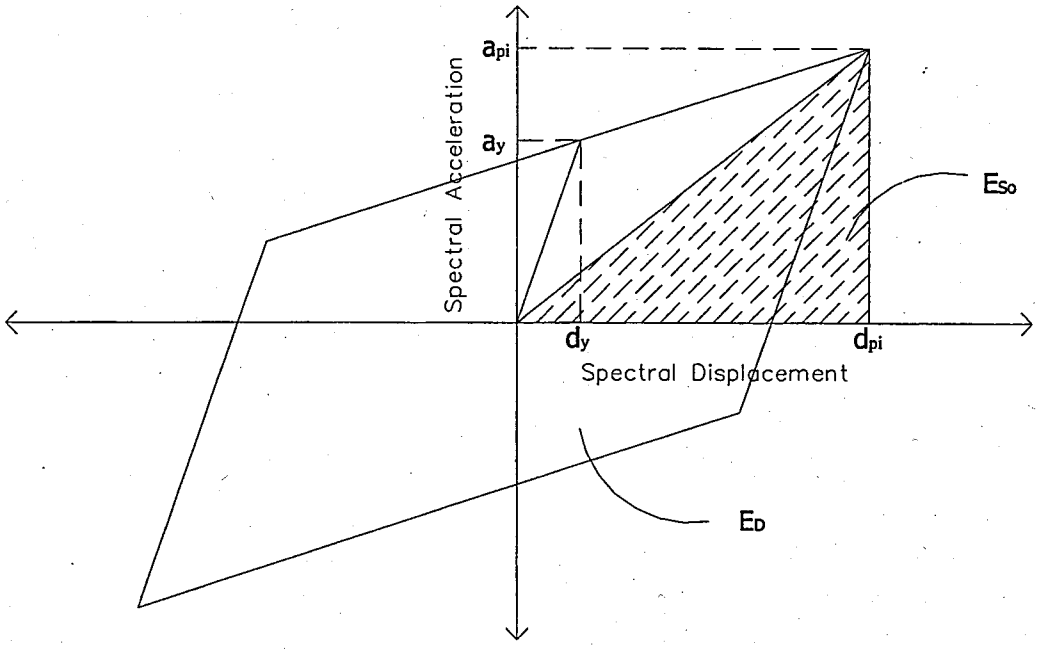

Figure 4.2. Derivation of damping for spectral reduction

The ranges and limits for the values of κ assigned to the three structural behavior types are given in Table 4.1. ATC 40 states that the formulas are derived from tables of spectrum reduction factors, B, specified for the design of base isolated buildings in the 1991 UBC, 1994 UBC and 1994 NEHRP Provisions.

4.3. Comparison of Effective Damping

Proper estimation of effective damping values is very imported in assessment of earthquake demand since spectral reduction factors are derived from these effective

damping values. A comparison is done between the effective damping values proposed by Kowalsky [5] and ATC 40 [7] for different displacement ductility ratios and setting bilinear stiffness ratio to 0.05. The results are given in Table 4.2 and illustrated in Figure 4.3. Effective damping values presented by ATC40 are taken as reference because the value of κ for structural behavior Type A (good behavior) is derived from the spectrum reduction factors specified in the Uniform Building Code (ICBO 1994) and the NEHRP Provisions (BSSC 1995) for the design of new isolated buildings. The values of κ assigned to the other two types are thought to be reasonable for average and poor structural behavior.

Table 4.1. Values for damping modification factor, κ

Structural Behavior Type	β_o (per cent)	K
Type A	≤16.25	1.0
	>16.25	$1.13-\frac{0.51(a_y d_{pi}-d_y a_{pi})}{a_{pi} d_{pi}}$
Type B	≤25	0.67
	>25	$0.845-\frac{0.446(a_y d_{pi}-d_y a_{pi})}{a_{pi} d_{pi}}$
Type C	Any Value	0.33

As can be seen from Table 4.2 and Figure 4.3 for low ductility levels the effective damping values proposed by direct displacement based design procedure is close to the ones proposed by ATC40 for structural behavior Type C. The effective damping values of DDBD are between ATC40 Type C and Type B structural behavior types for ductility ratios greater than 3 but always closer to Type C. In ATC40, Type C buildings are defined as poor existing buildings whose primary elements make up noncomplying lateral force systems with poor or unreliable hysteretic behavior or average existing buildings whose

primary elements are combinations of existing and new elements, or better than average existing systems but subjected to long shaking duration.

From the definition above it can be concluded that effective damping values presented by direct displacement based design procedure are very conservative since the range of this design procedure covers only new buildings. So, in this thesis effective damping values of ATC40 structural behavior Type B are used. Type B buildings are defined as essentially new buildings whose primary elements make up an essentially new lateral system and little strength or stiffness is contributed by noncomplying elements but the building is subjected to long shaking duration.

Table 4.2. Comparison of effective damping values

	β_{eff}			
μ	DDBD	ATC 40		
		TYPE A	TYPE B	TYPE C
1.25	8	17	13	9
1.50	10	24	18	11
2.00	13	31	24	15
3.00	17	36	27	17
4.00	19	37	27	18
6.00	21	37	27	18
8.00	22	37	27	18
10.00	22	37	27	17

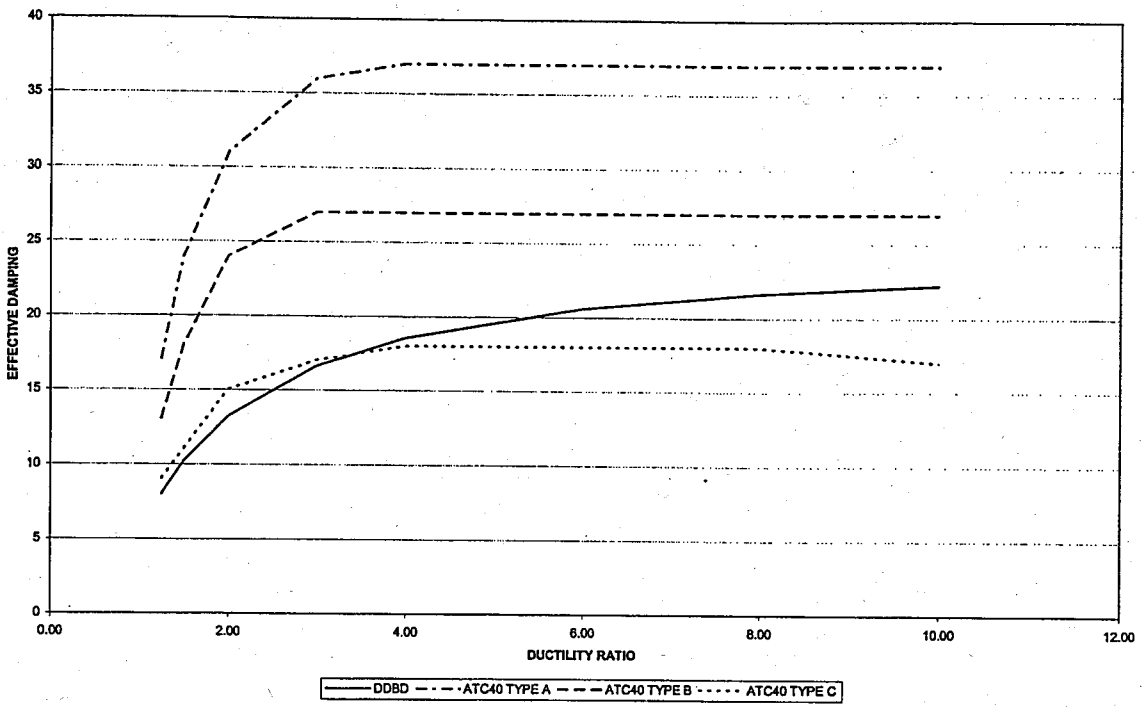

Figure 4.3. Comparison of effective damping values

5. REVISED DIRECT DISPLACEMENT BASED DESIGN

5.1. General

The response of reinforced concrete structures to strong earthquake motions is influenced by two basic phenomena: reduction in stiffness and increase in energy-dissipation capacity. As earthquake motion forces the structure to larger displacements, its stiffness decreases and its capacity to dissipate energy increases for the area within the hysteresis loop increases depending on displacement attained. Both effects can be related to ductility defined as the ratio of ultimate to yield displacement.

The direct displacement based design approach utilizes as its starting point a target displacement which is discussed in Chapter 2. Once the target displacement is defined substitute structure approach [3] is utilized to characterize the nonlinear behavior of an inelastic system with equivalent properties of effective stiffness and effective damping. The effective damping characteristics of a building can be obtained from ATC 40 [7] approach as stated in Chapter 4.

The seismic input for Direct Displacement-Based Design is expressed in the form of Acceleration-Displacement Response Spectra (ADRS). The spectral displacement values for the ADRS is obtained by multiplying spectral acceleration values of Standard Format (Sa vs T) Response Spectrum by $T^2 / 4\pi^2$

Capacity is a representation of the structure's ability to resist the seismic demand and capacity spectrum is obtained by dividing the horizontal ordinates of force-displacement curve by First Mode Participation Factor for top displacement (γ_n) and by dividing the vertical ordinates of force-displacement curve by Effective Participating Mass (M_e) which are given by Equations (5.1) and (5.2) respectively. Ψ_1 is the mode shape for the building and it is assumed to be an inverted triangle normalized to unity at the top storey.

$$\gamma_n = \Psi_{n1} * \left[\frac{\sum_{i=1}^{n} M_i * \Psi_{i1}}{\sum_{i=1}^{n} M_i * \Psi_{i1}^2} \right] \tag{5.1}$$

$$M_e = \gamma_n * m^* \tag{5.2}$$

$$m^* = \frac{1}{\Psi_{n1}} \sum_{i=1}^{n} M_i * \Psi_{i1} \tag{5.3}$$

Graphical representation of this conversion from equivalent force-displacement (capacity) curve to equivalent capacity spectrum is shown in Figure 5.1.

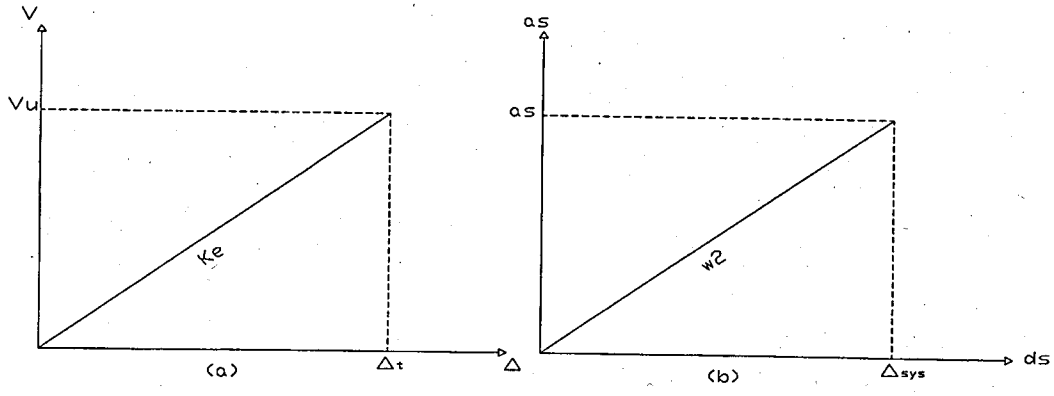

Figure 5.1. (a) Capacity curve ; (b) Capacity spectrum for substitute structure

Once the 5 per cent damped (elastic) response spectrum is converted to ADRS format, it is reduced by dividing ARS and DRS values with damping coefficients B_S or B_L depending on the period to obtain damped (inelastic) response spectrum.

$$B_S = \frac{2{,}12}{3{,}21 - 0{,}68 \ln(\beta_{eff})} \qquad \text{For Short Period } (T<T_B) \tag{5.4}$$

$$B_L = \frac{1{,}65}{2{,}31 - 0{,}41 \ln(\beta_{eff})} \qquad \text{For Long Period } (T>T_B) \tag{5.5}$$

For structural behavior type B β_{eff} values which are a function of slope ratio and ductility ratio are given in Table 5.1 [7].

Table 5.1. Effective damping in per cent for structural behavior type B

Ductility Ratio	Slope Ratio						
	0.5	0.4	0.3	0.2	0.1	0.05	0
10	9	10	12	16	23	27	29
8	9	11	13	17	24	27	29
6	10	12	15	19	25	27	29
4	11	14	17	21	25	27	29
3	12	14	17	21	25	27	29
2	12	14	16	19	22	24	25
1.5	11	12	14	15	17	18	18
1.25	9	10	10	11	12	13	13

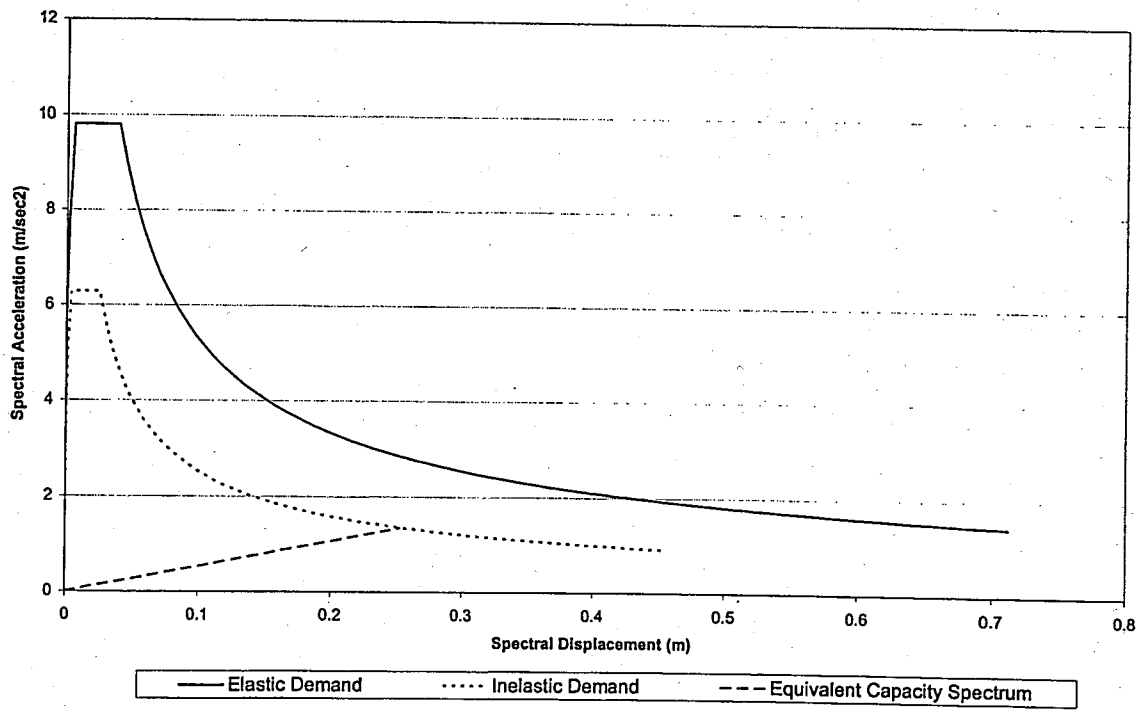

Figure 5.2. Demand and capacity spectrums

When the target spectral displacement is entered on the inelastic demand spectrum, performance point is readily obtained and the line which is drew from origin to performance point is the capacity spectrum for substitute structure. Ultimate base shear can be calculated either multiplying corresponding spectral acceleration by effective mass Me or multiplying target spectral displacement by effective stiffness.

$$V_u = Sa*Me \tag{5.6}$$

$$V_u = K_{eff}*\Delta_{sys} \tag{5.7}$$

Where, effective stiffness and effective period is given by Equations (5.8) and (5.9) respectively. ω^2 is the slope of the Equivalent Capacity Spectrum.

$$K_{eff} = \frac{4\pi^2}{T_{eff}^2} m_{eff} \tag{5.8}$$

$$T_{eff} = 2\pi / \omega \tag{5.9}$$

Design base shear is the yield base shear which can be calculated as the following:

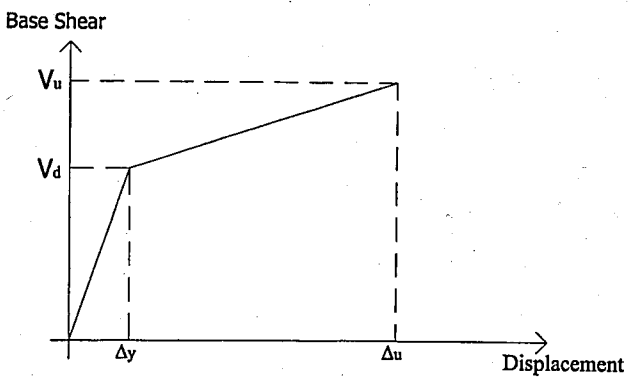

Figure 5.3. Idealized force displacement curve

If we designate the slope ratio as r then:

$$\frac{V_u - V_d}{\Delta_u - \Delta_y} = r\frac{V_d}{\Delta_y} \tag{5.10}$$

By rearranging the Equation (5.10),

$$\frac{1}{rV_d} = \frac{\Delta_u - \Delta_y}{\Delta_y (V_u - V_d)} \tag{5.11}$$

By setting Δ_u/Δ_y as ductility ratio,μ, the Equation (5.11) becomes,

$$\frac{1}{rV_d} = \frac{\mu - 1}{V_u - V_d} \tag{5.12}$$

Or conversely,

$$V_d = \frac{V_u}{r\mu - r + 1} \tag{5.13}$$

A series of structural wall building design examples are performed to explore the accuracy of design with regards to the pushover analyses practiced to designed buildings. The buildings of 4 stories are composed of structural walls of equal lengths. Each storey is 3m tall and the storey inertia weight is 950 KN/storey. Walls are uniformly 20cm thick Concrete compression strength is 25 Mpa. Longitudinal bar yield stress fy = 420 Mpa and longitudinal bar diameter d_{bl} = 14mm. The building is designed for seismic zone 1, Z2 type soil. (A_0=0,4 ; T_A= 0,15 sec ; T_B= 0,40 sec)

5.2. Building Design Composed 150x20 Structural Walls

For structural wall having section dimensions 150x20, target displacement profile was readily obtained in Chapter 3 which is given below:

For h_1 = 3m , Δ_1 = 0,058m

For h_2 = 6m , Δ_2 = 0,141m

For h_3 = 9m , Δ_3 = 0,238m

For h_4 = 12m , Δ_4 = 0,340m

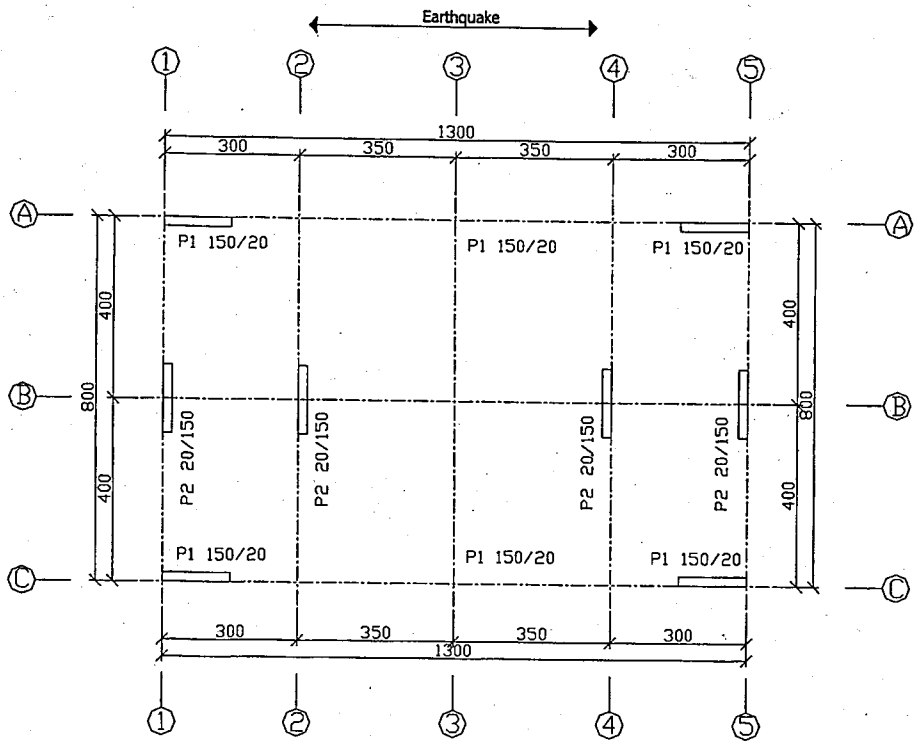

Figure 5.4. Plan view for building composed of 150x20 structural walls

Again from Chapter 3, elastic displacement profile is:

For $h_1 = 3m$, $\Delta_{e1} = 0{,}012m$

For $h_2 = 6m$, $\Delta_{e2} = 0{,}042m$

For $h_3 = 9m$, $\Delta_{e3} = 0{,}085m$

For $h_4 = 12m$, $\Delta_{e4} = 0{,}134m$

Displacement ductility ratio is then obtained from Equation (5.14)

$$\mu = \frac{\Delta_4}{\Lambda_{e4}} = \frac{0{,}340}{0{,}134} = 2.54 \qquad (5.14)$$

From Table 5.1 for ductility ratio 2.54 and slope ratio 0.05, the effective damping, β_{eff}, is 25.6, hence damping coefficients B_S and B_L are calculated as:

$$B_S = \frac{2{,}12}{3{,}21 - 0{,}68\ln(25.6)} = 2.11 \qquad \text{For Short Period (T<0.4)} \qquad (5.15)$$

$$B_L = \frac{1{,}65}{2{,}31 - 0{,}41\ln(25.6)} = 1.68 \qquad \text{For Long Period (T>0.4)} \qquad (5.16)$$

Inelastic response spectrum is the reduced acceleration-displacement response spectra, ADRS, with proportion to damping coefficients calculated above. First Mode Participation Factor for top displacement (γ_n) is calculated in Equation (5.17)

$$\gamma_n = 1 * \left[\frac{\sum_{i=1}^{n} 97 * (1 + 0.75 + 0.5 + 0.25 + 0)}{\sum_{i=1}^{n} 97 * (1^2 + 0.75^2 + 0.5^2 + 0.25^2 + 0^2)} \right] = 1.33 \qquad (5.17)$$

Target spectral displacement in other words system target displacement is then:

$$\Delta_{sys} = \frac{\Delta_4}{\gamma_n} = \frac{0.34}{1.33} = 0.26m \qquad (5.18)$$

When we enter the system target displacement to inelastic response spectrum, performance point is obtained and the equivalent capacity spectrum is drawn from origin to performance point which is shown in Figure 5.5. The vertical ordinate of the performance point is read as 0.80m/sn^2. Effective participating mass is calculated by (5.19) and ultimate base shear is given in (5.20).

$$M_e = 1.33 \frac{1}{1} \sum_{i=1}^{n} 97 * (1 + 0.75 + 0.50 + 0.25 + 0) = 320tons \qquad (5.19)$$

$$V_u = Sa*Me = 0.80*320 = 256KN \qquad (5.20)$$

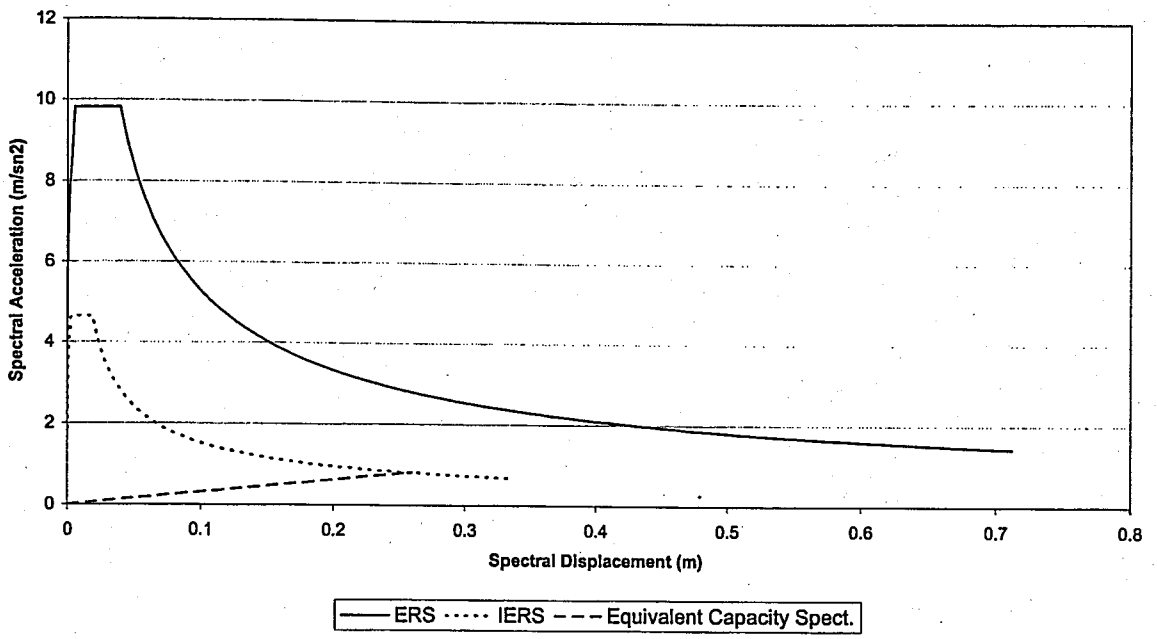

Figure 5.5. Response and capacity spectrums for building composed of 150x20 structural walls

Design base shear is the yield base shear, and for slope ratio 0.05 and ductility ratio 2.54 the design base shear is then:

$$V_d = \frac{256}{0.05*2.54-0.05+1} = 238KN \qquad (5.21)$$

5.3. Building Design Composed 300x20 Structural Walls

For structural wall having section dimensions 300x20, target displacement profile was readily obtained in Chapter 3 which is given below:

For $h_1 =$ 3m , $\Delta_1 = 0{,}052$m

For $h_2 =$ 6m , $\Delta_2 = 0{,}123$m

For $h_3 =$ 9m , $\Delta_3 = 0{,}201$m

For $h_4 =$ 12m , $\Delta_4 = 0{,}281$m

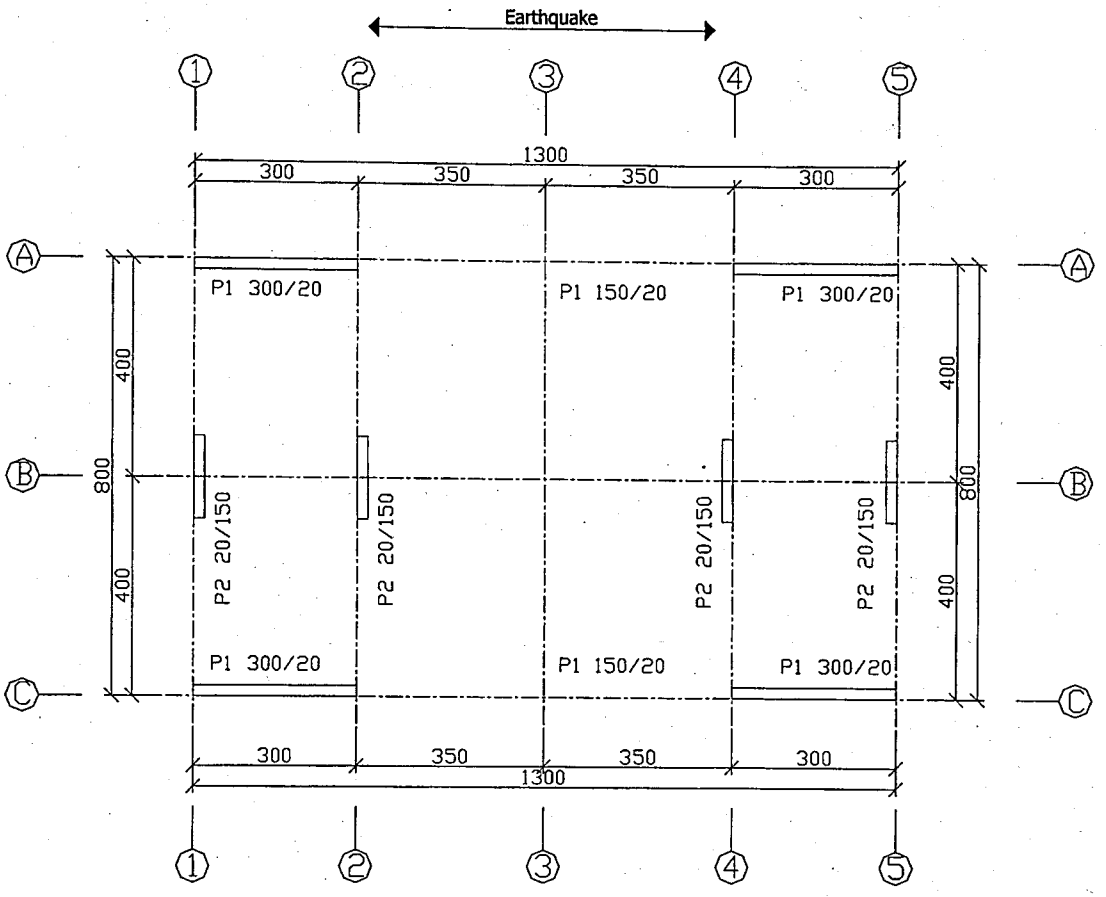

Figure 5.6. Plan view for building composed of 300x20 structural walls

Again from Chapter 3, elastic displacement profile is:

For $h_1 = 3m$, $\Delta_{e1} = 0{,}006m$

For $h_2 = 6m$, $\Delta_{e2} = 0{,}021m$

For $h_3 = 9m$, $\Delta_{e3} = 0{,}043m$

For $h_4 = 12m$, $\Delta_{e4} = 0{,}067m$

Displacement ductility is then obtained from Equation (5.22)

$$\mu = \frac{\Delta_4}{\Lambda_{e4}} = \frac{0{,}281}{0{,}067} = 4.19 \qquad (5.22)$$

From Table 5.1 for ductility ratio 4.19 and slope ratio 0.05, the effective damping, β_{eff}, is 27, hence damping coefficients B_S and B_L are calculated as:

$$B_S = \frac{2,12}{3,21 - 0,68\ln(27)} = 2.19 \qquad \text{For Short Period (T<0.4)} \qquad (5.23)$$

$$B_L = \frac{1,65}{2,31 - 0,41\ln(27)} = 1.72 \qquad \text{For Long Period (T>0.4)} \qquad (5.24)$$

Inelastic response spectrum is the reduced acceleration-displacement response spectra, ADRS, with proportion to damping coefficients calculated above. First Mode Participation Factor for top displacement (γ_n) is calculated in Equation (5.25)

$$\gamma_n = 1 * \left[\frac{\sum_{i=1}^{n} 97 * (1 + 0.75 + 0.5 + 0.25 + 0)}{\sum_{i=1}^{n} 97 * (1^2 + 0.75^2 + 0.5^2 + 0.25^2 + 0^2)} \right] = 1.33 \qquad (5.25)$$

Target spectral displacement in other words system target displacement is then:

$$\Delta_{sys} = \frac{\Delta_4}{\gamma_n} = \frac{0.28}{1.33} = 0.21m \qquad (5.26)$$

When we enter the system target displacement to inelastic response spectrum, performance point is obtained and the equivalent capacity spectrum is drawn from origin to performance point which is shown in Figure 5.7.

The vertical ordinate of the performance point is read as 0.87m/sn^2. Effective participating mass is calculated by (5.27) and ultimate base shear is given in (5.28).

$$M_e = 1.33 \frac{1}{1} \sum_{i=1}^{n} 97 * (1 + 0.75 + 0.50 + 0.25 + 0) = 320 tons \qquad (5.27)$$

$$V_u = Sa*Me=0.87*320=278KN \tag{5.28}$$

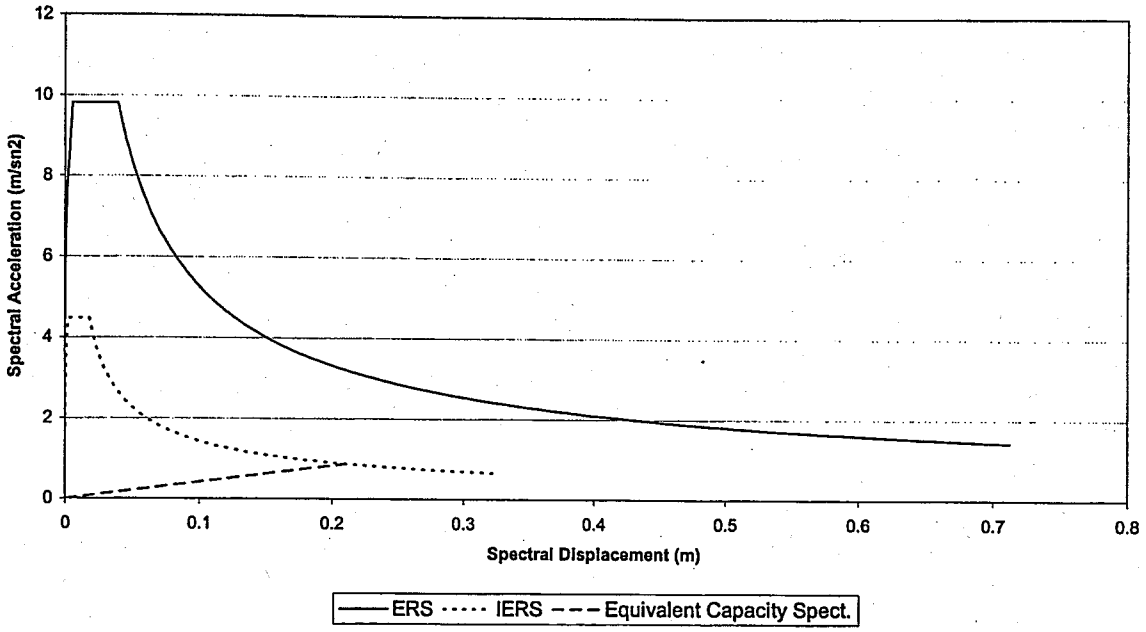

Figure 5.7. Response and capacity spectrums for building composed of 300x20 structural walls

Design base shear is the yield base shear, and for slope ratio 0.05 and ductility ratio 4.19 the design base shear is then:

$$V_{des} = \frac{278}{0.05*4.19-0.05+1} = 239KN \tag{5.29}$$

The design base shear calculated in Equation (5.29) is too small for a structural wall having length of 300cm so to provide a comparison between design and pushover analysis, the building is redesigned by increasing storey inertia weight to 3255 KN/storey. Hence the effective mass for the building is:

$$M_e = 1.33\frac{1}{1}\sum_{i=1}^{n} 332*(1+0.75+0.50+0.25+0) = 1103tons \tag{5.30}$$

Then the ultimate base shear is calculated from:

$$V_u = Sa*Me=0.87*1103=960KN \tag{5.31}$$

So, for slope ratio 0.05 and ductility ratio 4.19 the design base shear is then:

$$V_{des} = \frac{960}{0.05*4.19-0.05+1} = 828KN \tag{5.32}$$

5.4. Design Results and Conclusion

In the preceding sections, three building configurations have been designed. One was a building composed of 150x20 structural walls (Figure5.4) which will be referred as Design A and the other one was a building composed of 300x20 structural walls (Figure 5.6) which will be referred as Design B. Design C is identical with Design B but its storey inertia weight is set to 2000KN/storey to enable push over analysis on the building composed of 300x20 structural walls. The outputs for the designs A, B and C are summarized in Table 5.2.

Table 5.2. Summary of design results

Design Reference	Base Shear (KN)		Displacement Ductility	Effective Damping (%)	System Target Displacement (m)
	Design	Ultimate			
A	238	256	2.54	25.6	0.26
B	239	278	4.19	27.0	0.21
C	828	960	4.19	27.0	0.21

As can be seen from Table 5.2 displacement ductility ratios for design A and B are 2.54 and 4.19 respectively which means the ductility demand for the stiff structure is higher. This is expected since the yield curvature is directly affected from wall length; the yield curvature of a 300x20 structural wall is one half of the yield curvature of a 150x20 structural wall. That is why the elastic rotation, which is the integration of curvature along the plastic length, is smaller in stiff walls so, for the case 300x20 structural wall there is

more room for plastic rotation until total rotation reaches to limit state which in turn causes high ductility demand. Thus confinement detailing is more critical in stiff structural walls.

When we inspect ultimate base shears, we see that the ultimate base shear for structure B is higher despite the fact that with high ductility attained effective damping value is higher than that of structure A which in turn means higher damping coefficients. But as the system target displacement of structure B is lesser than structure A, the vertical ordinate of the performance point, which is spectral acceleration, is higher in structure B. Hence, ultimate base shear which is effective mass times spectral acceleration is higher in structure B. On the other hand, the design base shears of both structures are nearly equal. This is again because of the high ductility attained in structure B.

6. PUSHOVER ANALYSIS

6.1. General

In order to assess performance of the design procedure, pushover analyses are performed to the buildings designed in Sections 5.2. and 5.3.

The analyzed buildings are of 4 stories and they are composed of structural walls of equal lengths. Each storey is 3m tall. The storey inertia weight is 950 KN/storey for building composed of 150x20 structural walls and 2000 KN/storey for building composed of 300x20 structural walls. Walls are uniformly 20cm thick Concrete compression strength is 25 MPa. Longitudinal bar yield stress fy = 420 MPa and longitudinal bar diameter d_{bl} = 14mm. The building is designed for seismic zone 1, Z2 type soil. (A_0 =0,4 ; T_A= 0,15 sec ; T_B= 0,40 sec)

Structural walls are modeled according to enhanced equivalent column model which is reviewed in Chapter 3. To simulate the global building response equivalent columns are constrained to each other. The design base shear is distributed along the stories assuming that first mode shape is the inverted triangle. Reinforcement content for the structural walls is selected so that their yield strengths are identical with the ones of design to provide conformity with design and analysis. Directional properties of SAP2000 NLLink elements and modification factors for frame sections are calculated according to results obtained from moment-curvature analyses.

Once the system is constructed it is pushed with inverted triangle loading normalized to unity. Displacement values for top storey and base moments formed in the NLLINK elements are noted. System is further pushed until the step 1 base moment of any of the individual NLLINK element reaches to structural wall yield moment which is found from moment-curvature analysis. An amplification factor α_1 is calculated from (6.1) and all values (top displacement and base shear) noted in step 1 are multiplied with α_1. The directional properties of plastified NLLink are changed with its post-yield properties and system is reanalyzed for the inverted triangle loading normalized to unity. α_2 is the

required amplification factor for the next NLLink element to reach its yield moment and is given by (6.2).

$$\alpha_1 = \frac{M_y}{M_1} \tag{6.1}$$

$$\alpha_2 = \frac{M_y - M_1\alpha_1}{M_2} \tag{6.2}$$

Pushover continues until the system becomes unstable and for each α_i factor top displacement and base shear values are calculated to construct force-displacement curve in other words push-over curve.

$$d_i = d_1\alpha_1 + d_2\alpha_2 + \ldots\ldots + d_i\alpha_i \tag{6.3}$$

$$V_i = V_1\alpha_1 + V_2\alpha_2 + \ldots\ldots + V_i\alpha_i \tag{6.4}$$

d_i : top displacement for i^{th} step

V_i : base shear for i^{th} step

Once push-over curve is built, it is converted to capacity spectrum by dividing the horizontal ordinates of force-displacement curve by First Mode Participation Factor for top displacement ,γ_n, and by dividing the vertical ordinates of force-displacement curve by Effective Participating Mass, M_e. Capacity spectrum is plotted on the same chart with 5 per cent damped (elastic) response spectrum converted to ADRS format. In first iteration trial performance points are selected to be the end point of the capacity spectrum and spectral reduction factors are calculated.

When the spectral reduction factors are calculated, demand spectrum can be plotted and the intersection of the capacity spectrum and demand spectrum is our new performance point. Since the area bounded with capacity spectrum and performance point is changed reduction factors changed, so we plot new demand spectra reduced with new

reduction factors. This process is repeated until the displacement $d_{p(i+1)}$ is within 5 per cent of displacement d_{pi}, then the point $a_{p(i+1)}$, $d_{p(i+1)}$ is the final performance point.

Base moments for each NLLink element are calculated at where the system is pushed to final performance point. Since we know the elastic and plastic rotational stiffness' of NLLink elements total rotations can be calculated from (6.5).

$$\theta_T = \frac{M_y}{R_{3y}} + \frac{M_p - M_y}{R_{3py}} \tag{6.5}$$

Where,

M_y: Yield moment of structural wall

M_p: Total moment of structural wall when the system is displaced to performance point

R_{3y}: Pre-yield rotational stiffness for NLLink element

R_{3py}: Post-yield rotational stiffness for NLLink element

6.2. Pushover Analysis for Building Composed of 150x20 Structural Walls

For the building given in Figure 6.1 contributions of perpendicular walls are neglected and walls parallel to earthquake direction are modeled according to enhanced equivalent column model in Sap2000 [8]. As stated in Chapter 3, enhanced equivalent column model is appropriate for the purposes of this thesis, and simulating non-linear behavior of a structural system is easily maintained by this equivalent model.

For the inverted triangle loading normalized to unity at top displacement, base shear is 0.625 KN and base moment is 5.37 KNm for each of the structural walls. Since our design base shear, which was found in Chapter 5, is 238 KN; for building composed of 150x20 structural walls in the earthquake direction the amplification factor is then:

$$\alpha_1 = \frac{238}{4*0.625} = 95 \tag{6.6}$$

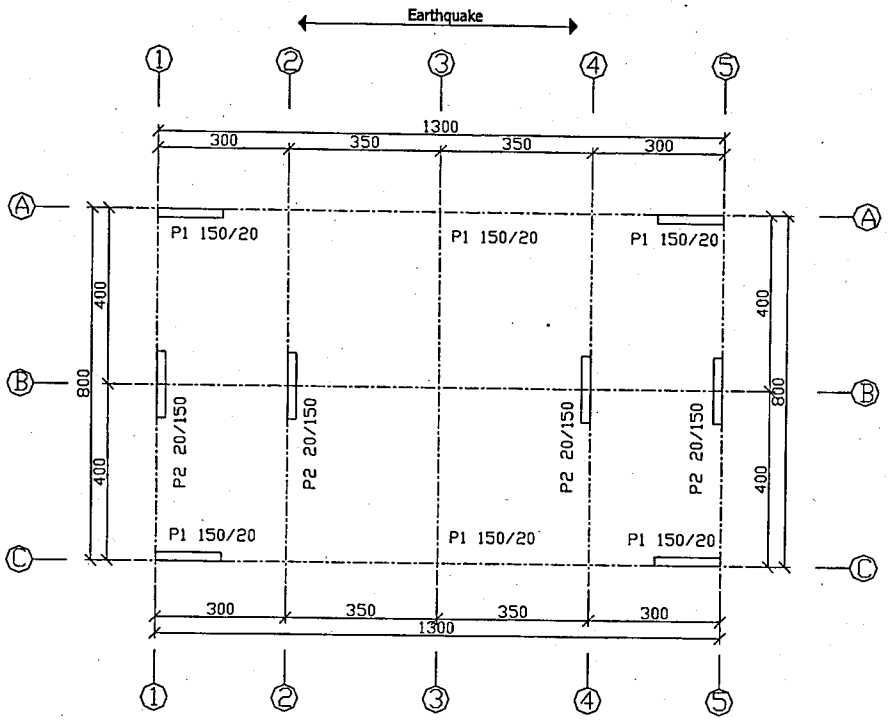

Figure 6.1. Plan view for building composed of 150x20 structural walls

By rearranging Equation (6.1) yield base moment is calculated by Equation (6.7).

$$M_y = M_1\alpha_1 = 5.37*95 = 510KNm \tag{6.7}$$

To maintain conformity with analysis and design a 150x20 structural wall which is effective yield moment is 510 KNm is designed.

According to Figure 6.2 EI effective is 2.08E+5 KN-m^2 and yield EI effective is 5.82E+2 KN-m^2. Hence, the calculated modification factors and NLLink directional properties are given in Table 6.1.

Pre-yield modification factors and NLLink directional properties are reentered and the system is pushed with inverted triangle loading normalized to unity at top storey. Top storey displacement is read as 1.17E-3 m and elastic top storey displacement is then:

$$\Delta_{et} = 1.17E-3*95 = 0.11m \tag{6.8}$$

Table 6.1. Modification factors and NLLink directional properties for 150x20 structural wall

	EI Effective KN-m2	I Effective m4	Ig m4	M.F.	R3 KN-m	U2 KN/m
Preyield	2.08E+05	6.93E-03	5.63E-02	0.1233	2.60E+05	4.88E+06
Postyield	5.82E+02	1.94E-05	5.63E-02	0.0003	7.28E+02	1.36E+04

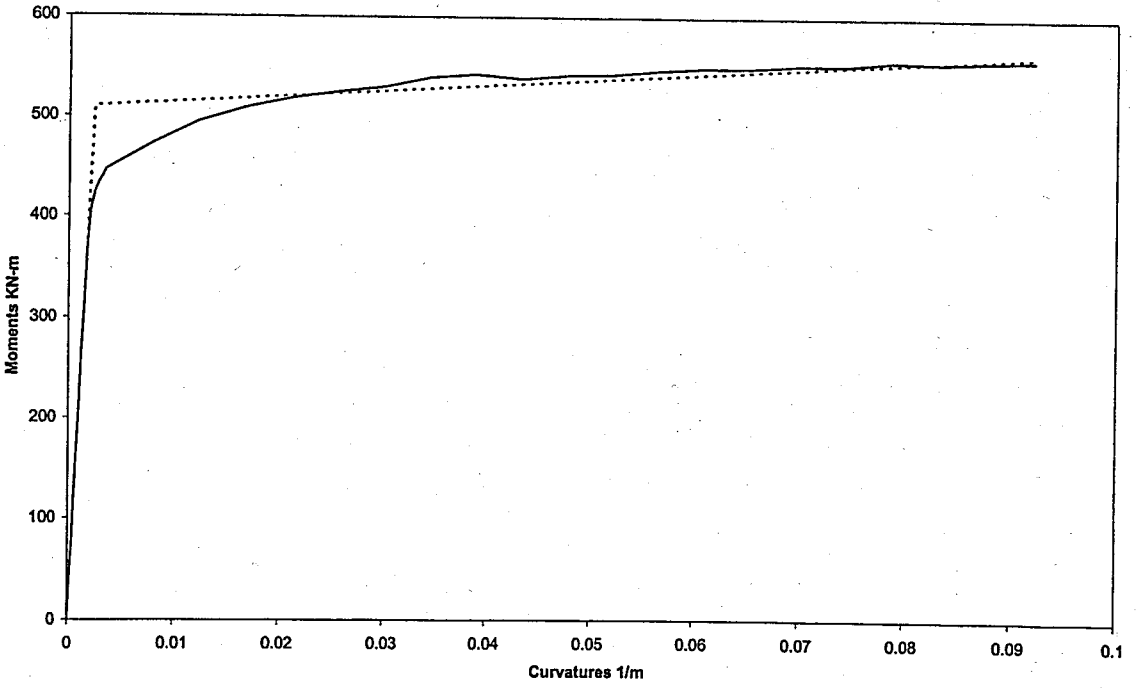

Figure 6.2. Moment-Curvature relationship for 150x20 structural wall

Once the elastic top storey is found, post-yield NLLink directional properties are entered to the model and system is again pushed with inverted triangle loading normalized to unity at top storey. The top storey displacement is 0.0933m; base shear and base moment for each of the structural walls are 0.625KN and 5.37 KNm respectively. For ultimate moment 562 KNm, the amplification factor α_2 is given by Equation (6.9)

$$\alpha_2 = \frac{M_u - M_1\alpha_1}{M_2} = \frac{562-510}{5.37} = 9.7 \tag{6.9}$$

Ultimate base shear is calculated from:

$$V_u = 4*(V_1\alpha_1 + V_2\alpha_2) = 4*(0.625*95 + 0.625*9.7) = 262KN \tag{6.10}$$

Ultimate displacement is given by:

$$\Delta u = \Delta_1\alpha_1 + \Delta_2\alpha_2 = 1.17E-3*95 + 9.33E-2*9.7 = 1.02m \tag{6.11}$$

Force displacement curve is plotted for the structure and it is converted to capacity spectrum by dividing the horizontal ordinates of force-displacement curve by First Mode Participation Factor for top displacement, γ_n, and by dividing the vertical ordinates of force-displacement curve by Effective Participating Mass, M_e. By assuming the first mode shape as inverted triangle normalized to unity at top storey γ_n is found by Equation (6.12).

$$\gamma_n = 1*\left[\frac{\sum_{i=1}^{n} 97*(1+0.75+0.5+0.25+0)}{\sum_{i=1}^{n} 97*(1^2+0.75^2+0.5^2+0.25^2+0^2)}\right] = 1.33 \tag{6.12}$$

Effective participating mass is given by Equation (6.13), taking storey inertia mass 97 tons.

$$M_e = 1.33\frac{1}{1}\sum_{i=1}^{n} 97*(1+0.75+0.50+0.25+0) = 320tons \tag{6.13}$$

Spectral yield displacement and ultimate spectral displacement are given by Equations (6.14) and (6.15).

$$S_{dy} = \frac{\Delta_y}{\gamma_n} = \frac{0.11}{1.33} = 0.083m \tag{6.14}$$

$$S_{du} = \frac{\Delta_u}{\gamma_n} = \frac{1.02}{1.33} = 0.767m \tag{6.15}$$

Spectral yield acceleration and ultimate spectral acceleration are calculated by Equations (6.16) and (6.17).

$$S_{ay} = \frac{V_y}{M_e} = \frac{238}{320} = 0.74m/sn^2 \tag{6.16}$$

$$S_{au} = \frac{V_u}{M_e} = \frac{262}{320} = 0.82m/sn^2 \tag{6.17}$$

Force displacement curve and capacity spectrum are illustrated in Figure 6.3 and Figure 6.4 respectively.

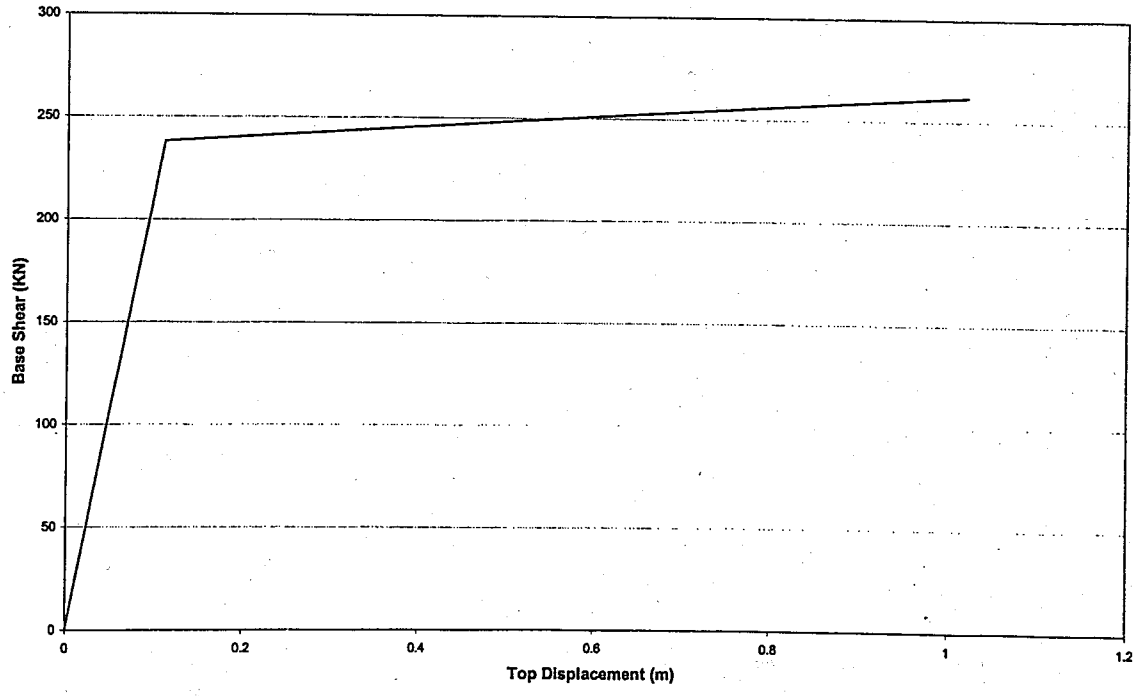

Figure 6.3. Force-displacement curve for structure composed of 150x20 structural walls

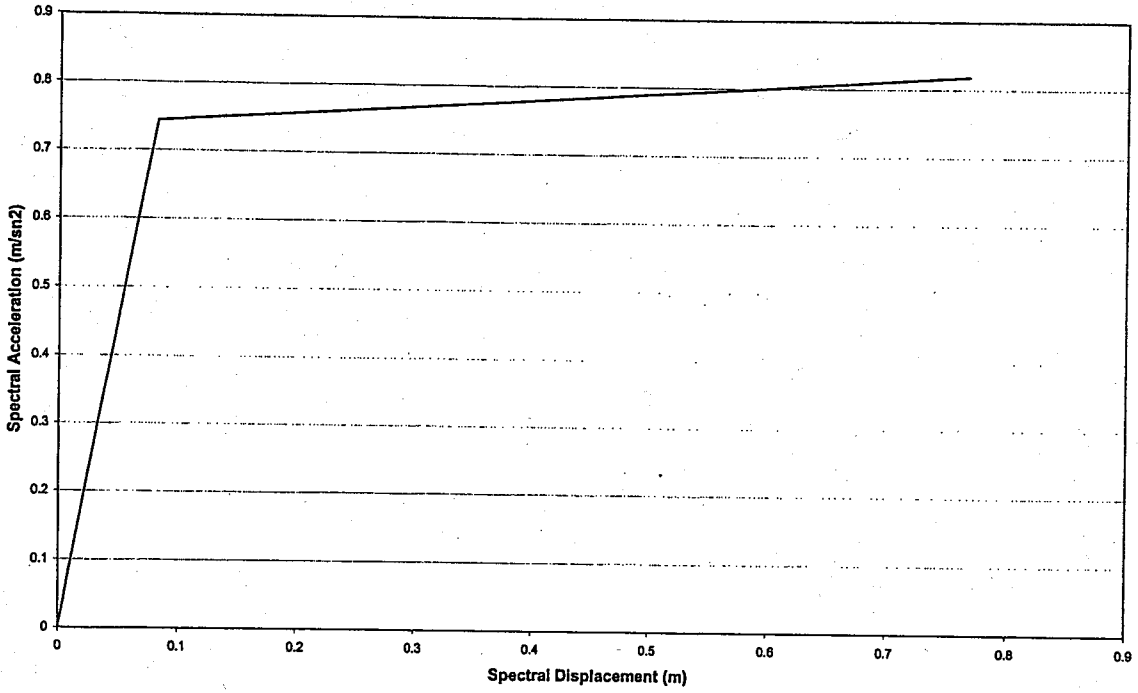

Figure 6.4. Capacity spectrum for structure composed of 150x20 structural walls

In the first iteration spectral displacement and spectral acceleration for the first trial performance point is selected as 0.29m and 0.77m/sn^2 respectively according to equal displacement approximation. Hysteretic damping is then calculated from Equation (6.18) which is given by ATC40 where, S_{di} is the spectral displacement and S_{ai} is the spectral acceleration for the performance point selected.

$$\beta_0 = \frac{0.637(S_{ay}S_{di} - S_{dy}S_{ai})}{S_{ai}S_{di}} = \frac{0.637(0.74*0.29 - 0.083*0.77)}{0.77*0.29} = 43\% \qquad (6.18)$$

For hysteretic damping, β_0, greater than 25 per cent, damping modification factor, κ, is:

$$\kappa = 0.845 - \frac{0.446(S_{ay}S_{di} - S_{dy}S_{ai})}{S_{ai}S_{di}} \qquad (6.19)$$

$$\kappa = 0.845 - \frac{0.446(0.74*0.29 - 0.083*0.77)}{0.77*0.29} = 0.54$$

Effective viscous damping, β_{eff}, is then:

$$\beta_{eff} = \kappa\beta_0 + 5 = 0.54 * 43 + 5 = 28.2\% \tag{6.20}$$

Hence damping coefficients B_S and B_L are calculated as:

$$B_S = \frac{2,12}{3,21 - 0,68\ln(28.2)} = 2.26 \qquad \text{For Short Period (T<0.4)} \tag{6.21}$$

$$B_L = \frac{1,65}{2,31 - 0,41\ln(28.2)} = 1.75 \qquad \text{For Long Period (T>0.4)} \tag{6.22}$$

Elastic response spectrum converted to ADRS format is reduced with damping coefficients calculated above and is plotted on the same chart with capacity spectrum.

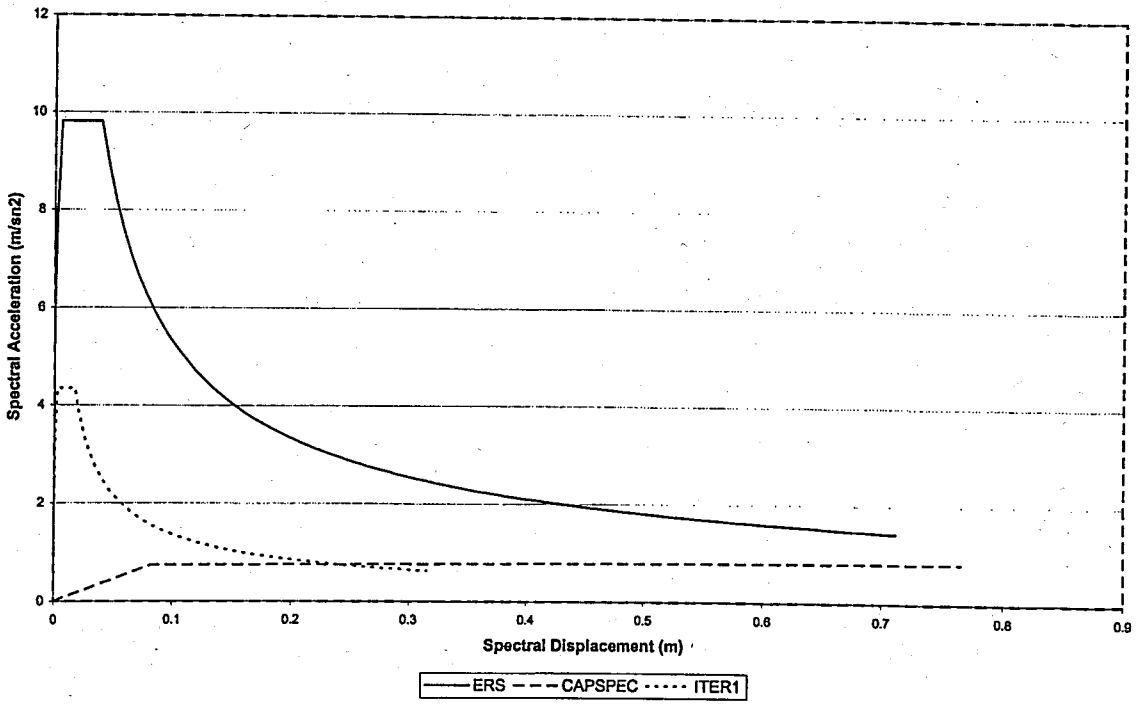

Figure 6.5. First iteration demand and response spectrums for building composed of 150x20 structural walls

As can be seen from Figure 6.5 our new performance point is the intersection of inelastic response spectrum and capacity spectrum. Spectral displacement of the

performance point is read as 0.236m and spectral displacement is read as 0.761 m/sn^2. Hence effective damping for the second iteration is:

$$\beta_0 = \frac{0.637(S_{ay}S_{di} - S_{dy}S_{ai})}{S_{ai}S_{di}} = \frac{0.637(0.74*0.236 - 0.083*0.761)}{0.761*0.236} = 39\% \quad (6.23)$$

For hysteretic damping, β_0, greater than 25 per cent, damping modification factor, κ, is:

$$\kappa = 0.845 - \frac{0.446(S_{ay}S_{di} - S_{dy}S_{ai})}{S_{ai}S_{di}} \quad (6.24)$$

$$\kappa = 0.845 - \frac{0.446(0.74*0.236 - 0.083*0.761)}{0.761*0.236} = 0.57$$

Effective viscous damping, β_{eff}, is then:

$$\beta_{eff} = \kappa\beta_0 + 5 = 0.57*39 + 5 = 27.2\% \quad (6.25)$$

Therefore damping coefficients B_S and B_L are calculated as:

$$B_S = \frac{2,12}{3,21 - 0,68\ln(27.2)} = 2.20 \qquad \text{For Short Period (T<0.4)} \quad (6.26)$$

$$B_L = \frac{1,65}{2,31 - 0,41\ln(27.2)} = 1.73 \qquad \text{For Long Period (T>0.4)} \quad (6.27)$$

Figure 6.6 represents the updated inelastic demand spectrum together with the inelastic demand spectrum found from iteration 1.

Spectral displacement of the performance point is read as 0.253m and spectral displacement is read as 0.760 m/sn^2. Therefore hysteretic damping for the third iteration is:

$$\beta_0 = \frac{0.637(S_{ay}S_{di} - S_{dy}S_{ai})}{S_{ai}S_{di}} = \frac{0.637(0.74*0.253 - 0.083*0.760)}{0.760*0.253} = 41\% \qquad (6.28)$$

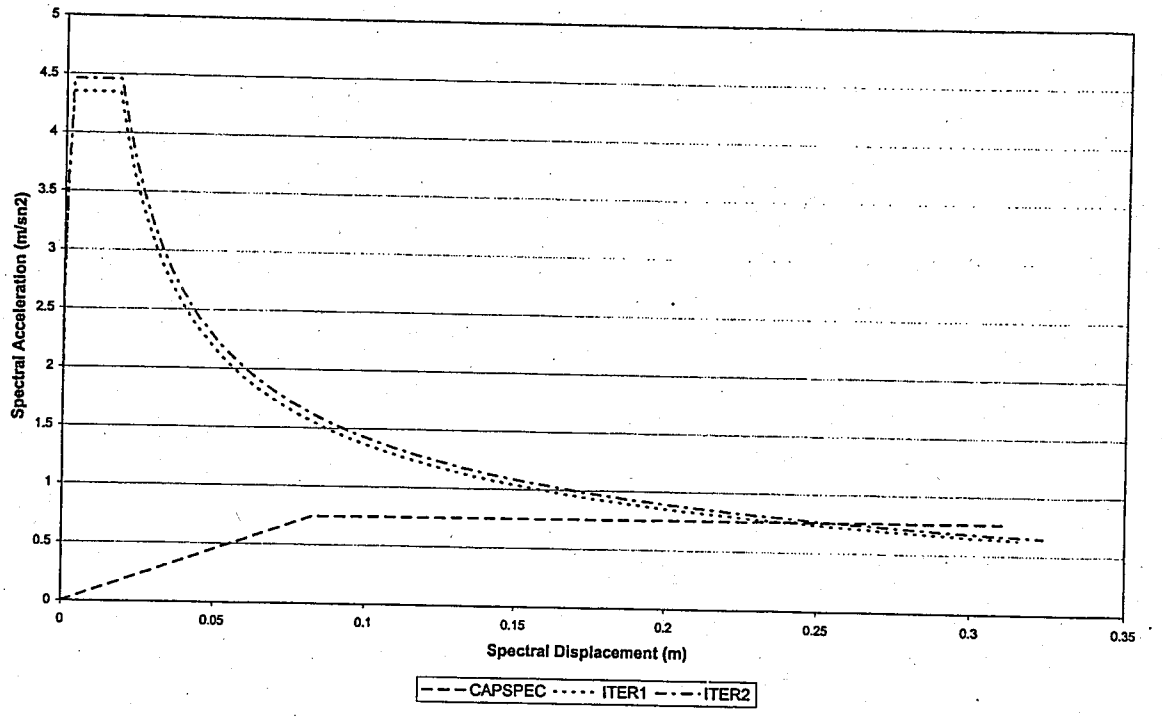

Figure 6.6. Second iteration demand and response spectrums for building composed of 150x20 structural walls

For hysteretic damping, β_0, greater than 25 per cent, damping modification factor, κ, is:

$$\kappa = 0.845 - \frac{0.446(S_{ay}S_{di} - S_{dy}S_{ai})}{S_{ai}S_{di}} \qquad (6.29)$$

$$\kappa = 0.845 - \frac{0.446(0.74*0.253 - 0.083*0.760)}{0.760*0.253} = 0.56$$

Effective viscous damping, β_{eff}, is then calculated by:

$$\beta_{eff} = \kappa\beta_0 + 5 = 0.56*41 + 5 = 28\% \qquad (6.30)$$

So, damping coefficients B_S and B_L are calculated as:

$$B_S = \frac{2,12}{3,21 - 0,68\ln(28)} = 2.24 \qquad \text{For Short Period (T<0.4)} \qquad (6.31)$$

$$B_L = \frac{1,65}{2,31 - 0,41\ln(28)} = 1.75 \qquad \text{For Long Period (T>0.4)} \qquad (6.32)$$

According to Figure 6.7 for third iteration spectral displacement for performance point is 0.242m and spectral acceleration is 0.763m/sn^2. Since the deviation between performance points from iterations 2 and 3 is 4 per cent, third iteration performance point is the final performance point.

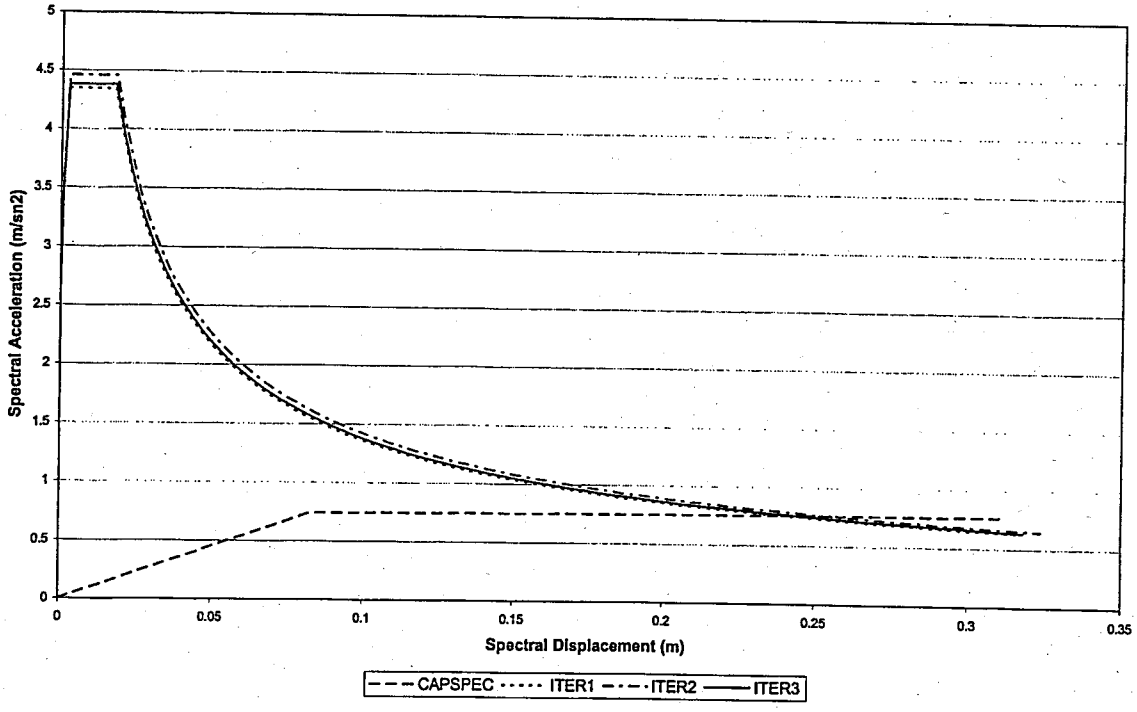

Figure 6.7. Third iteration demand and response spectrums for building composed of 150x20 structural walls

The base shear at which the building is displaced to performance point is given by Equation (6.33).Where S_{ap} is the spectral displacement at performance point and M_e is the effective mass.

$$V_p = S_{ap} * M_e = 0.763 * 320 = 244KN \tag{6.33}$$

The amplification factor at which the building is pushed until performance point is calculated by Equation (6.34)

$$\alpha_p = \frac{V_p - V_y}{4 * V_1} = \frac{244 - 238}{4 * 0.625} = 2.4 \tag{6.34}$$

Base moment at performance point is then:

$$M_p = M_1\alpha_1 + M_2\alpha_p = 5.37 * 95 + 5.37 * 2.4 = 523KNm \tag{6.35}$$

So, total rotation of the plastic hinge is given by Equation (6.36)

$$\theta_T = \frac{M_y}{R_{3y}} + \frac{M_p - M_y}{R_{3py}} = \frac{510}{2.6E+5} + \frac{523 - 510}{7.28E+2} = 0.0198rad \tag{6.36}$$

6.3. Pushover Analysis for Building Composed of 300x20 Structural Walls

For the building given in Figure 6.8 contributions of perpendicular walls are neglected and walls parallel to earthquake direction are modeled according to enhanced equivalent column model in Sap2000 [8].

For the inverted triangle loading normalized to unity at top displacement, base shear is 0.625 KN and base moment is 5.31 KNm for each of the structural walls. Since our design base shear, which was found in Chapter 5, is 828 KN; for building composed of 300x20 structural walls in the earthquake direction the amplification factor is then:

$$\alpha_1 = \frac{828}{4 * 0.625} = 331 \tag{6.37}$$

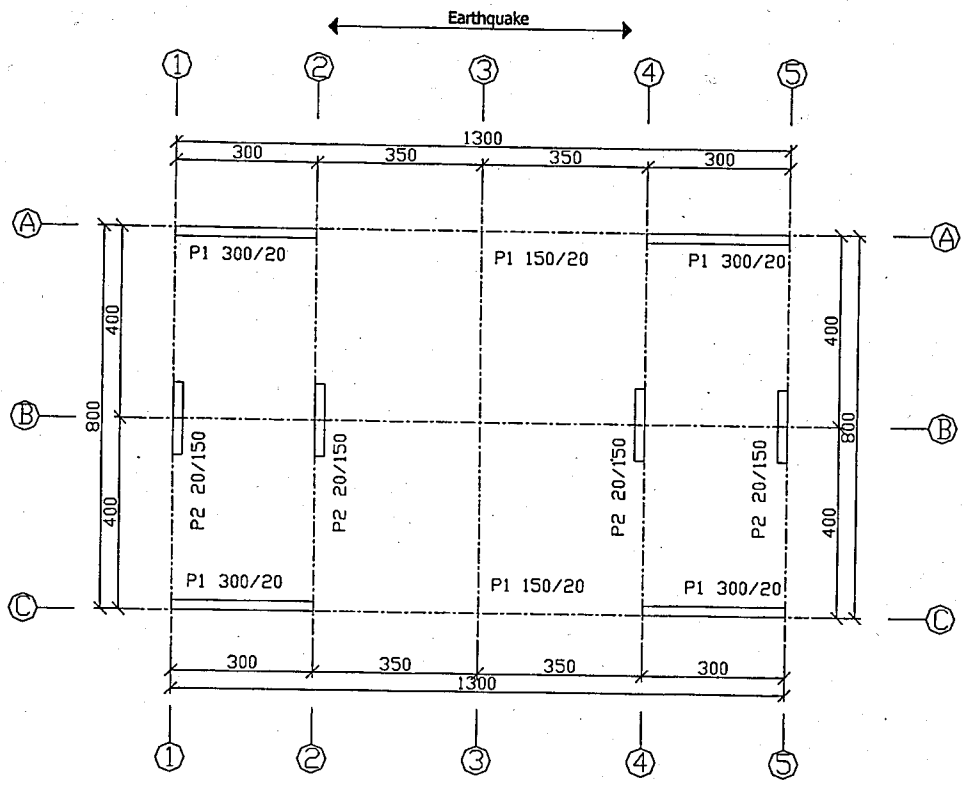

Figure 6.8. Plan view for building composed of 300x20 structural walls

By rearranging Equation (6.1) yield base moment is calculated by Equation (6.7).

$$M_y = M_1 \alpha_1 = 5.31 * 331 = 1758 KNm \tag{6.38}$$

To maintain conformity with analysis and design a 300x20 structural wall which is effective yield moment is 1758 KNm is designed.

According to Figure 6.9 EI effective is 1.41E+06 KN-m^2 and yield EI effective is 4.28E+03 KN-m^2. Hence, the calculated modification factors and NLLink directional properties are given in Table 6.1.

Pre-yield modification factors and NLLink directional properties are reentered and the system is pushed with inverted triangle loading normalized to unity at top storey. Top storey displacement is read as 1.74E-4m and elastic top storey displacement is then:

$$\Delta_{el} = 1.74E-4*331 = 0.058m \quad (6.39)$$

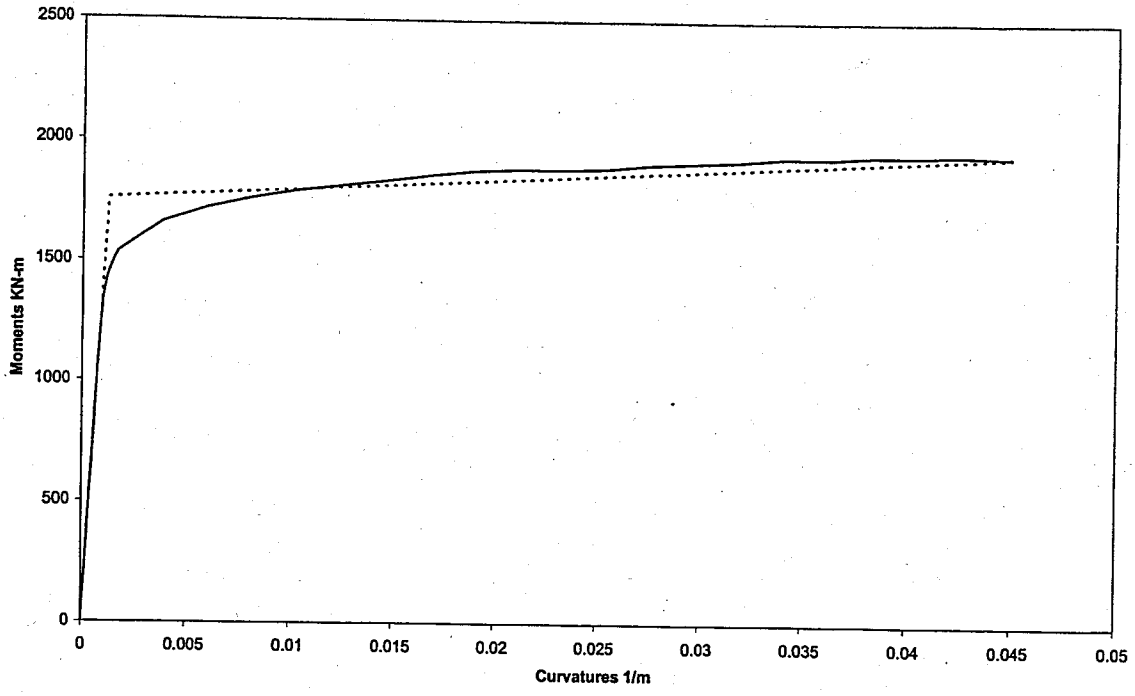

Figure 6.9. Moment-Curvature relationship for 300x20 structural wall

Table 6.2. Modification factors and NLLink directional properties for 300x20 structural wall

	EI Effective KN-m2	I Effective m4	Ig m4	M.F.	R3 KN-m	U2 KN/m
Preyield (Elastic)	1.41E+06	4.70E-02	4.50E-01	0.1044	1.41E+06	1.69E+07
Postyield	4.28E+03	1.43E-04	4.50E-01	0.0003	4.28E+03	5.14E+04

Once the elastic top storey is found, post-yield NLLink directional properties are entered to the model and system is pushed with inverted triangle loading normalized to unity at top storey. The top storey displacement is 0.0159 m; base shear and base moment for each of the structural walls are 0.625KN and 5.37 KNm respectively. For ultimate moment 1945 KNm, the amplification factor α_2 is given by Equation (6.40)

$$\alpha_2 = \frac{M_u - M_1\alpha_1}{M_2} = \frac{1945-1758}{5.31} = 35.2 \tag{6.40}$$

Ultimate base shear is calculated from:

$$V_u = 4*(V_1\alpha_1 + V_2\alpha_2) = 4*(0.625*331 + 0.625*35.2) = 915KN \tag{6.41}$$

Ultimate displacement is given by:

$$\Delta u = \Delta_1\alpha_1 + \Delta_2\alpha_2 = 1.74E-4*331 + 1.59E-2*35.2 = 0.62m \tag{6.42}$$

Force displacement curve is plotted for the structure and it is converted to capacity spectrum by dividing the horizontal ordinates of force-displacement curve by First Mode Participation Factor for top displacement, γ_n, and by dividing the vertical ordinates of force-displacement curve by Effective Participating Mass, M_e. By assuming the first mode shape as inverted triangle normalized to unity at top storey γ_n is found by Equation (6.43).

$$\gamma_n = 1*\left[\frac{\sum_{i=1}^{n} 332*(1+0.75+0.5+0.25+0)}{\sum_{i=1}^{n} 332*(1^2+0.75^2+0.5^2+0.25^2+0^2)}\right] = 1.33 \tag{6.43}$$

Effective participating mass is given by Equation (6.44), taking storey inertia mass 332 tons.

$$M_e = 1.33\frac{1}{1}\sum_{i=1}^{n} 332*(1+0.75+0.50+0.25+0) = 1104tons \tag{6.44}$$

Spectral yield displacement and ultimate spectral displacement are given by Equations (6.14) and (6.15).

$$S_{dy} = \frac{\Delta_y}{\gamma_n} = \frac{0.058}{1.33} = 0.044m \tag{6.45}$$

$$S_{du} = \frac{\Delta_u}{\gamma_n} = \frac{0.62}{1.33} = 0.47m \tag{6.46}$$

Spectral yield acceleration and ultimate spectral acceleration are calculated by Equations (6.16) and (6.17).

$$S_{ay} = \frac{V_y}{M_e} = \frac{828}{1104} = 0.75m/sn^2 \tag{6.47}$$

$$S_{au} = \frac{V_u}{M_e} = \frac{915}{1104} = 0.83m/sn^2 \tag{6.48}$$

Force displacement curve and capacity spectrum are illustrated in Figure 6.10 and Figure 6.11 respectively.

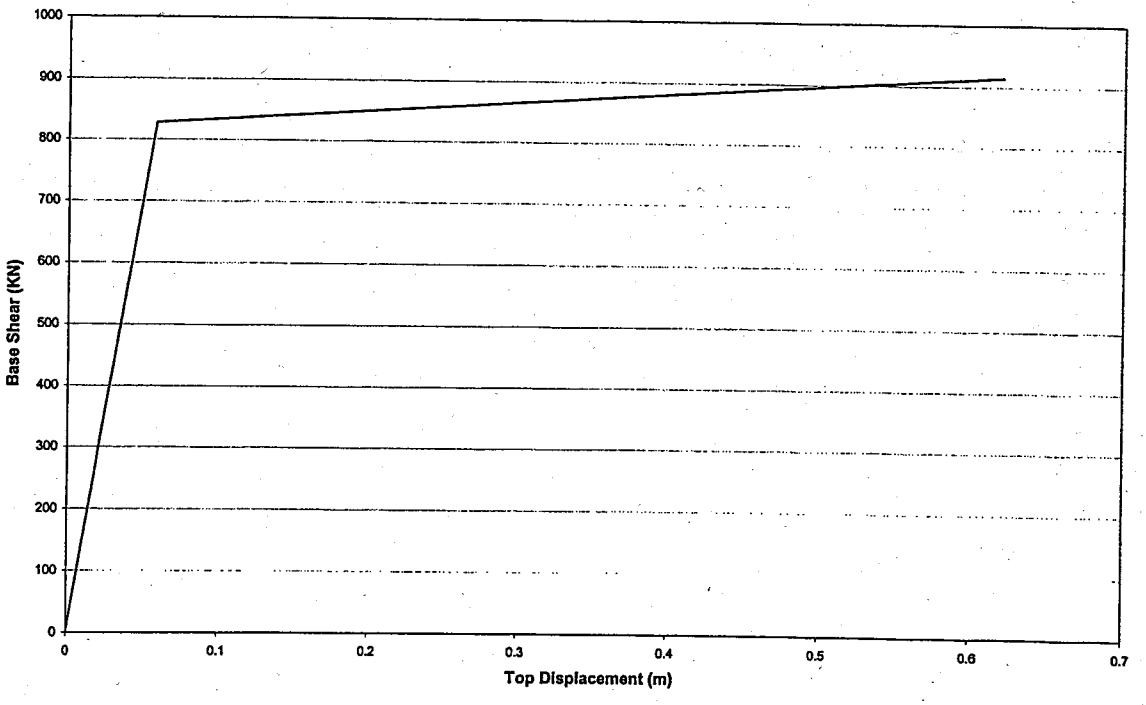

Figure 6.10. Force-displacement curve for structure composed of 300x20 structural walls

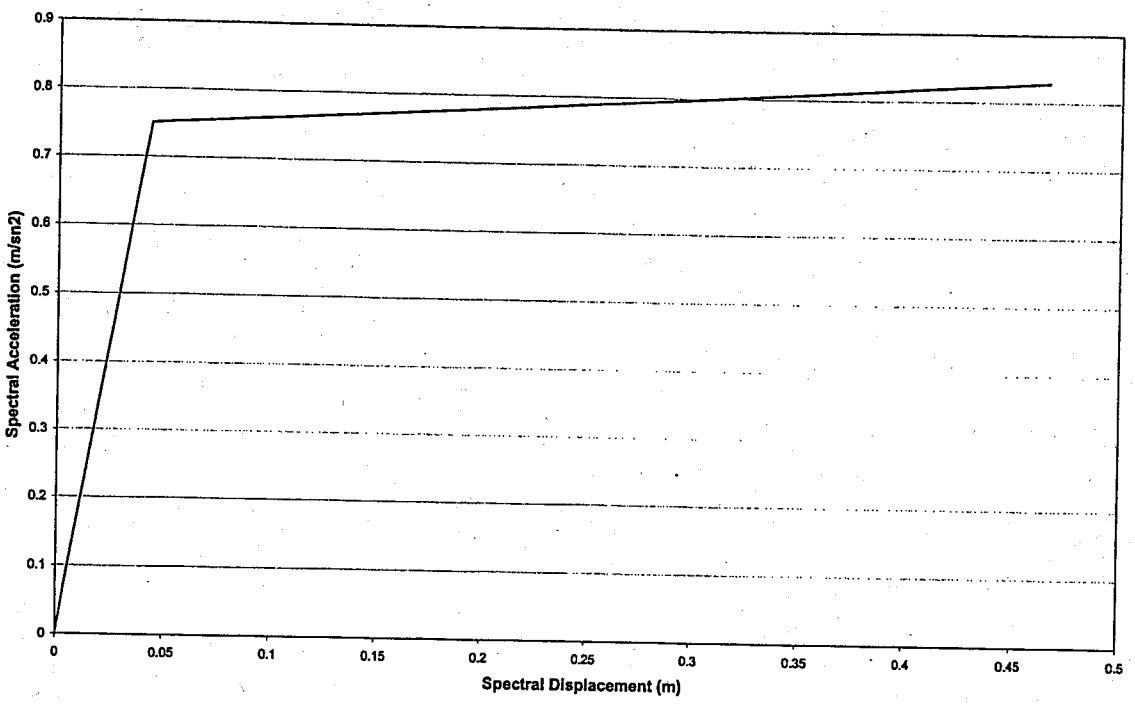

Figure 6.11. Capacity spectrum for structure composed of 300x20 structural walls

In the first iteration spectral displacement and spectral acceleration for the first trial performance point is selected as 0.19m and 0.78m/sn^2 respectively according to equal displacement approximation. Hysteretic damping is then calculated from Equation (6.49) which is given by ATC40 where, S_{di} is the spectral displacement and S_{ai} is the spectral acceleration for the performance point selected.

$$\beta_0 = \frac{0.637(S_{ay}S_{di} - S_{dy}S_{ai})}{S_{ai}S_{di}} = \frac{0.637(0.75*0.19 - 0.044*0.78)}{0.78*0.19} = 46\% \qquad (6.49)$$

For hysteretic damping, β_0, greater than 25 per cent, damping modification factor, κ, is:

$$\kappa = 0.845 - \frac{0.446(S_{ay}S_{di} - S_{dy}S_{ai})}{S_{ai}S_{di}} \qquad (6.50)$$

$$\kappa = 0.845 - \frac{0.446(0.75*0.19 - 0.044*0.78)}{0.78*0.19} = 0.52$$

Effective viscous damping, β_{eff}, is then:

$$\beta_{eff} = \kappa\beta_0 + 5 = 0.52 * 46 + 5 = 28.9\% \tag{6.51}$$

Hence damping coefficients B_S and B_L are calculated as:

$$B_S = \frac{2{,}12}{3{,}21 - 0{,}68\ln(28.9)} = 2.30 \qquad \text{For Short Period (T<0.4)} \tag{6.52}$$

$$B_L = \frac{1{,}65}{2{,}31 - 0{,}41\ln(28.9)} = 1.77 \qquad \text{For Long Period (T>0.4)} \tag{6.53}$$

In ATC 40 maximum value for B_S is defined as 2.27 for structural behavior type B, so B_S value is set to 2.27. Elastic response spectrum converted to ADRS format is reduced with damping coefficients calculated above and is plotted on the same chart with capacity spectrum.

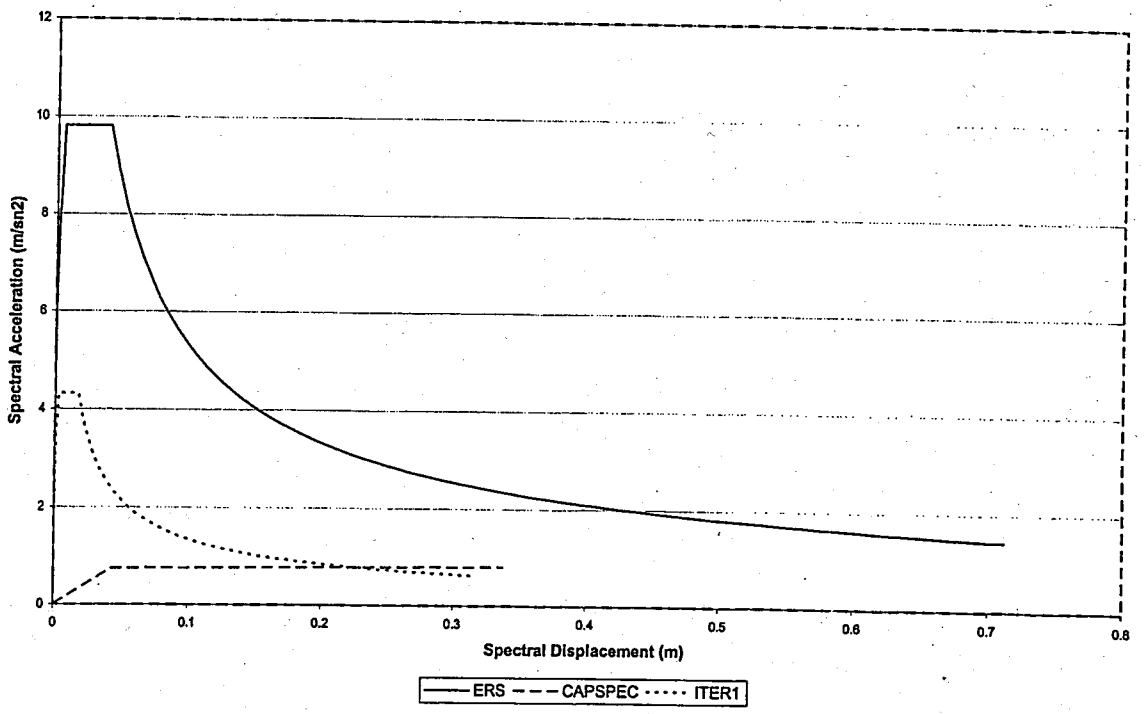

Figure 6.12. First iteration demand and response spectrums for building composed of 300x20 structural walls

As can be seen from Figure 6.12 our new performance point is the intersection of inelastic response spectrum and capacity spectrum. Spectral displacement of the performance point is read as 0.23 m and spectral displacement is read as 0.78 m/sn^2. Hence effective damping for the second iteration is:

$$\beta_0 = \frac{0.637(S_{ay}S_{di} - S_{dy}S_{ai})}{S_{ai}S_{di}} = \frac{0.637(0.75*0.23 - 0.044*0.78)}{0.78*0.23} = 49\% \qquad (6.54)$$

For hysteretic damping, β_0, greater than 25 per cent, damping modification factor, κ, is:

$$\kappa = 0.845 - \frac{0.446(S_{ay}S_{di} - S_{dy}S_{ai})}{S_{ai}S_{di}} \qquad (6.55)$$

$$\kappa = 0.845 - \frac{0.446(0.74*0.23 - 0.044*0.78)}{0.78*0.23} = 0.51$$

Effective viscous damping, β_{eff}, is then:

$$\beta_{eff} = \kappa\beta_0 + 5 = 0.51*49 + 5 = 30.0\% \qquad (6.56)$$

Therefore damping coefficients B_S and B_L are calculated as:

$$B_S = \frac{2{,}12}{3{,}21 - 0{,}68\ln(30.0)} = 2.36 \qquad \text{For Short Period (T<0.4)} \qquad (6.57)$$

$$B_L = \frac{1{,}65}{2{,}31 - 0{,}41\ln(30.0)} = 1.80 \qquad \text{For Long Period (T>0.4)} \qquad (6.58)$$

In ATC 40 maximum value for B_S is defined as 2.27 and B_L is defined as 1.79 for structural behavior type B, so B_S and B_L values are set to 2.27 and 1.79 respectively.

Figure 6.13 represents the updated inelastic demand spectrum together with the inelastic demand spectrum found from iteration 1.

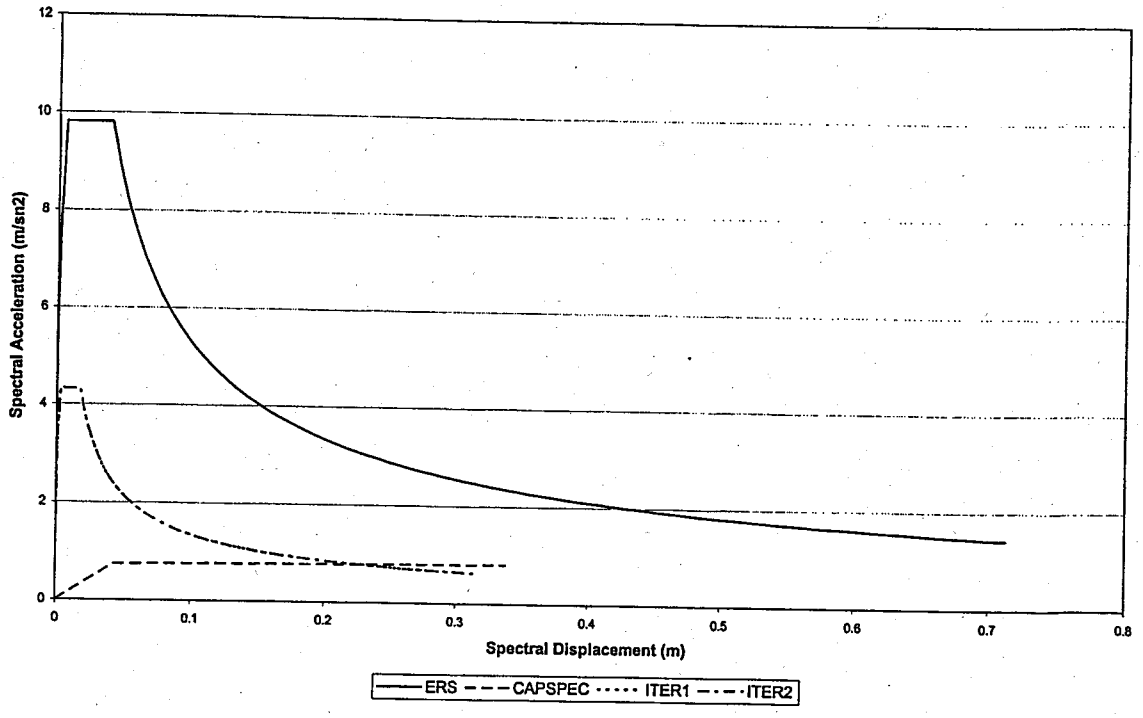

Figure 6.13. Second iteration demand and response spectrums for building composed of 300x20 structural walls

Spectral displacement of the performance point is read as 0.223 m and spectral displacement is read as 0.784 m/sn^2. Since the deviation between performance points from iterations 1 and 2 is 3 per cent, third iteration performance point is the final performance point.

The base shear at which the building is displaced to performance point is given by Equation (6.59).Where S_{ap} is the spectral displacement at performance point and M_e is the effective mass.

$$V_p = S_{ap} * M_e = 0.784 * 1104 = 865KN \tag{6.59}$$

The amplification factor at which the building is pushed until performance point is calculated by Equation (6.60)

$$\alpha_p = \frac{V_p - V_y}{4 * V_1} = \frac{865 - 828}{4 * 0.625} = 14.8 \tag{6.60}$$

Base moment at performance point is then:

$$M_p = M_1\alpha_1 + M_2\alpha_p = 5.31 * 331 + 5.31 * 14.8 = 1836 KNm \tag{6.61}$$

So, total rotation of the plastic hinge is given by Equation (6.62)

$$\theta_T = \frac{M_y}{R_{3y}} + \frac{M_p - M_y}{R_{3py}} = \frac{1758}{1.41E+6} + \frac{1836 - 1758}{4.28E+3} = 0.0195 rad \tag{6.62}$$

6.4. Comparison of Design and Analysis Results

When formulating target displacement profile it was seen that yield curvature is a function of wall length, so elastic displacement profile is different for various structural wall sections. To better understand the effects of wall length in the design procedure 150cm and 300cm length structural walls were considered.

While evaluating the acceptability of design, two criteria are considered: (1) conformity in system target displacement, (2) conformity in total rotation in plastic zones. Pushover analysis results in terms of total rotation in plastic zone are so that they perfectly match the design total rotation limit. Deviation is only 1 per cent for building composed of 150x20 structural walls and 2.5 per cent for 300x20 structural wall building.

When we look at system target displacements, we see similar agreement with design and analysis results. Error is 7 per cent and 6 per cent for buildings composed of 150x20 and 300x20 structural walls respectively. Divergence is probably due to the estimated elastic displacement profile and due to deviation from presumed slope ratio of 0.05.

7. CONCLUSIONS AND RECOMMENDATIONS

The objective of the displacement-based design is to provide a rational seismic design based on a pre selected performance level. There are two key points in the design procedure, which are: (1) A mathematical model to estimate target displacement profile; (2) an effective damping as a measure of energy dissipated through hysteresis loops. A procedure for displacement-based design presented by Kowalsky [5] was examined and it was seen that the original mathematical model used in estimation of target displacement profile leads designer to elastic design for especially slender walls. Also effective damping was found to be conservative when compared to ATC40 procedure so, ATC40 proposed effective damping values were used. Original mathematical model in estimating target displacement profile was revised by setting the total rotation that takes place in plastic zone as design restraint. Target displacement profile was than reformulated to snap shot the top storey displacement at the instant of limit rotation at base. To assess the goals of design, a series of designs and analyses were performed on structural wall buildings with various wall section configurations. The outcomes are as the following:

i. Target displacement profile suggested by Kowalsky [5] includes elastic rotations at top storey level which is proportional to the wall height. For higher wall aspect ratios this top storey elastic rotation increases so that there is left limited room for plastic rotation within a specified drift limit. Therefore, ductility ratio decreases to an extent that it becomes an elastic design for high wall aspect ratios. For this reason yield base shear increases as stiffness decreases, which is in direct contrast to code proposed demand spectrum.

ii. For a given section dimensions, variation in strength in other words reinforcement content has almost no effect on displacement profile of the wall and total rotation in plastic zone. However it is seen that, target displacement profile estimation in walls having greater lengths is closer to the actual deformation pattern.

iii. Effective damping values proposed by Kowalsky [5] are conservative and they generally match Type C buildings which are defined as poor existing buildings by ATC40 [7]. Therefore, effective damping values for Type B buildings, which are new buildings subjected to long shaking duration, are used.

iv. There is a direct relation between wall length and ductility demand. Ductility demand of walls having higher lengths is greater so confinement detailing is more critical in such walls.

v. The design results are in tolerable limits with respect to pushover analysis results but relatively high divergence in terms of system target displacement stems from error in estimation of elastic displacement profile. Since mathematical model for estimating elastic displacement profile is based on the double integration of curvature along the wall height, a more detailed work on curvature is recommended.

REFERENCES

1. Gülkan, P. and M. Sözen, "Inelastic Response of Reinforced Concrete Structures to Earthquake Motions" *ACI Journal of the American Concrete Institute*, Vol. 71, No. 12, pp. 601-609, Dec. 1974.

2. Takeda, T., M. Sözen and N. N. Nielsen, "Reinforced Concrete Response to Simulated Earthquakes" *Journal of the Structural Division,* ASCE, Vol. 96, No. ST12, pp. 2557-2573, Dec. 1970.

3. Shibata, A. and M. Sözen, "Substitute Structure Method for Seismic Design in R/C" *Journal of the Structural Division,* ASCE, Vol. 102, No.1, pp. 1-18, Jan. 1976.

4. Kowalsky, M. J., M. J. N. Priestley and G. A. MacRae, "Displacement-Based Design of RC Bridge Columns in Seismic Regions" *Earthquake Engineering and Structural Dynamics,* Vol. 24, No. 12, pp. 1623-1642, June 1995.

5. Kowalsky, M. J., "RC Structural Walls Designed According to UBC and Displacement-Based Methods" *Journal of Structural Engineering,* ASCE, Vol. 127, No. 5, pp. 506-516, May 2001.

6. Paulay, T. and M. J. N. Priestley, *Seismic Design of Reinforced Concrete and Masonry Buildings,* Wiley, New York, 1992.

7. Applied Technology Council, *ATC-40 Seismic Evaluation and Retrofit of Concrete Buildings*, Volume 1, ATC, Redwood City, California, 1996.

8. SAP 2000, "Structural Analysis Program", http://www.csiberkeley.com

REFERENCES NOT CITED

Bachmann, H. and A. Dazio, "A Deformation-Based Seismic Design Procedure for Structural Wall Buildings" *Proceedings of the International Workshop on Seismic Design Methodologies for the Next Generation Codes*, pp. 1-12, June 1997.

Kongoli, X., T. Minami and Y. Sakai, "Effects of Structural Walls on the Elastic-Plastic Earthquake Responses of Frame-Wall Buildings" *Earthquake Engineering and Structural Dynamics,* Vol. 28, pp. 479-500, 1999.

Mehanny, S.S.F., H. Kuramoto and G. G. Deierlein, "Stiffness Modeling of Reinforced Concrete Beam-Columns for Frame Analysis" *ACI Structural Journal,* Vol. 98, No.2, pp. 215-225, April 2001.

Panagiotakos, T. B. and M. N. Fardis, "A Displacement Based Seismic Design Procedure for RC Buildings and Comparison with EC8" *Earthquake Engineering and Structural Dynamics,* Vol. 30, pp. 1439-1462, 2001.

Silva, M. A. and C. C. Swan, "Failure Criterion for RC Members Under Biaxial Bending and Axial Load" *Journal of Structural Engineering,* ASCE, Vol. 127, No. 8, pp. 922-929, August 2001.

Wallace, J. W., "Seismic Design of RC Structural Walls. Part I: New Code Format" *Journal of Structural Engineering,* ASCE, Vol. 121, No. 1, pp. 75-87, Jan. 1995.

Wallace, J. W. and J. H. Thomsen, "Seismic Design of RC Structural Walls. Part II: Applications" *Journal of Structural Engineering,* ASCE, Vol. 121, No. 1, pp. 88-101, Jan. 1995.

Ziemian, R. D. and W. McGuire, "Modified Tangent Modulus Approach, a Contribution to Plastic Hinge Analysis" *Journal of Structural Engineering,* ASCE, Vol. 128, No. 10, pp. 1301-1307, Oct. 2002.